4

ORNL-2470 cy 4
Reactors - General

SAFEGUARD REPORT FOR A STAINLESS STEEL RESEARCH REACTOR FOR THE BSF (BSR-II)

E. G. Silver
J. Lewin

OAK RIDGE NATIONAL LABORATORY
operated by
UNION CARBIDE CORPORATION
for the
U.S. ATOMIC ENERGY COMMISSION

ORNL-2470
Reactors-General

Copy No. ________

Contract No. W-7405-eng-26

NEUTRON PHYSICS DIVISION

SAFEGUARD REPORT FOR A STAINLESS STEEL RESEARCH REACTOR FOR THE BSF (BSR-II)

E. G. Silver and J. Lewin*

DATE ISSUED

JUL 16 1958

OAK RIDGE NATIONAL LABORATORY
Oak Ridge, Tennessee
operated by
UNION CARBIDE CORPORATION
for the
U.S. ATOMIC ENERGY COMMISSION

*On assignment from The Martin Company, Baltimore 3, Maryland.

TABLE OF CONTENTS

ABSTRACT

An additional reactor, to be designated as the BSR-II, is proposed for the ORNL Bulk Shielding Facility. This reactor is to be a light water-moderated, convection-cooled, pool-type, research reactor, consisting of stainless steel-clad, plate-type fuel elements and using a cermet of highly enriched UO_2 and stainless steel as fuel. The BSR-II is to be used alternatively with the present aluminum-clad reactor (BSR-I). It is to be supported by the same support structure and is also to use the same control circuitry and radiation detectors. The BSR-II is to be a 15-in.-cube core, containing about 6 kg of 93% enriched U^{235} in 25 fuel elements, each having 20 plates. The plates are to have an 8-mil-thick cladding and a 14-mil-thick fuel region. The BSR-II is designed to operate at 750 kw and have an element lifetime of 10 to 15 years.

Calculations indicate that the prompt neutron lifetime will be of the order of 25 μsec. The control system will be adequate to reverse periods of the order of 10 msec.

To eliminate any credible accidental excursions severe enough to constitute a hazard, a limitation of 0.7% on excess reactivity (which limits periods to 100 msec) is proposed. Within this limitation there exists no credible accident which would result in the release of fission-product activity into the atmosphere, either due to a reactor

excursion, or from a melt-down due to afterheat in case of coolant loss.

This report contains a description of the mechanical features and the dimensions of the reactor, the nuclear and heat transfer characteristics as calculated, and a discussion of the proposed control system, including the results of experimental investigations of the proposed control system and its dynamic behavior. The site description and discussions of geological and security considerations pertaining to the BSR-II have been adequately presented in safeguard reports[1-3] for other reactors at ORNL and will not, in general, be discussed in this report.

A series of tests of the BSR-II is planned for the SPERT facility, with a view to possible increases in permissible excess reactivity and reactor power. If such increases seem justified further Safeguard Committee approval will be requested.

INTRODUCTION

Since the construction of the Bulk Shielding Reactor (BSR-I) in 1950, it has been highly successful as a research reactor and has served as the prototype for many other reactors. This widespread interest in pool-type reactors has prompted the design of a modified version of this reactor type which will retain the simplicity, low cost, and experimental flexibility of the BSR-I, but will add some improved features to help overcome the limitations of the present design. It is proposed that this new reactor, to be identified as the BSR-II, be built and operated at the Bulk Shielding Facility.

The greatest improvement in the new design will be the increased life of the fuel elements, which are to be clad with stainless steel. The useful life of the presently used aluminum-clad fuel elements is limited by corrosion of the aluminum in water. The life is observed to be of the order of two to four years, whereas from the neutron economy viewpoint a much longer service might be expected. It is anticipated that a stainless steel-clad fuel element might withstand corrosion for 10 or 15 years under similar conditions. This longer life would be particularly advantageous in reactors intended for applications where fuel reprocessing and fabrication is less readily available than at a national laboratory.

The development of the stainless steel fuel-element fabrication technology has made it possible to design such a reactor for the BSF, where it is to be used for experiments related to shielding development. The reactors for which optimized shields must be designed have, in many cases, core components of nickel, chrome, and iron, and the gamma-ray spectrum from such a core is much better approximated for shield test purposes by a stainless steel core than by an aluminum one.

The opportunity of designing a new core for the BSF was used to attain a more compact and symmetric shape for the core. This is desirable for the interpretation of many shield penetration experiments, where a small and simple source geometry lends itself more readily to the analysis of the results. It is also advantageous in permitting smaller, lighter, and more compact wrap-around experimental shields to be used.

It is hoped that the building and operation of such a reactor, incorporating relatively short neutron generation times, will lead to increased understanding of reactor kinetics in pool-type reactors.

The design of the reactor was subject to specific criteria which governed the decisions involved. These criteria are:

1. The reactor is to be used alternatively with the BSR-I, and it is to use the same support structure, control circuits, and control panels.

2. The core should, as discussed above, be as compact and symmetric as other considerations permit.
3. Techniques presently developed for fabrication of stainless steel fuel elements are to be applied as far as possible (i.e., techniques developed for the first Army Package Power Reactor (APPR-I)).
4. The handling, loading, storage and manipulation of the fuel elements for the BSR-II should be similar to the well developed techniques used for the BSR-I fuel elements.

I. DESIGN OF THE REACTOR

The possibility of designing a 1-ft-cube core, consisting of 16 elements in a 12-in.-high square array, was briefly considered and discarded on several grounds, including short neutron lifetime, high fuel inventory, and highly epithermal neutron spectrum. The design effort was then concentrated on a 15-in.-cube core, consisting of 25 elements in a 5 by 5 array.

In agreement with the desirability of a small and compact geometry, the grid plate (Fig. 1) was designed to hold no more than the 25 elements called for in the design, rather than the much larger number possible with the BSR-I. However, the elements can be inserted in two orientations, which will yield flexibility in control plate location, as will be discussed below. This grid plate, which will be constructed of type 17-7 stainless steel, will be used in the modified BSF support structure as shown in Fig. 2. It is to be placed in position with the aid of the two dowel pins shown and attached by means of four screws as indicated in the drawing.

The fuel elements are designed as shown in Fig. 3. It will be observed that the elements each contain 20 flat plates of the familiar sandwich construction. The fuel material is a cermet consisting of UO_2 ($\approx$25 wt %) and stainless steel ($\approx$75 wt %). The side plates and the

UNCLASSIFIED
2-01-058-0-329

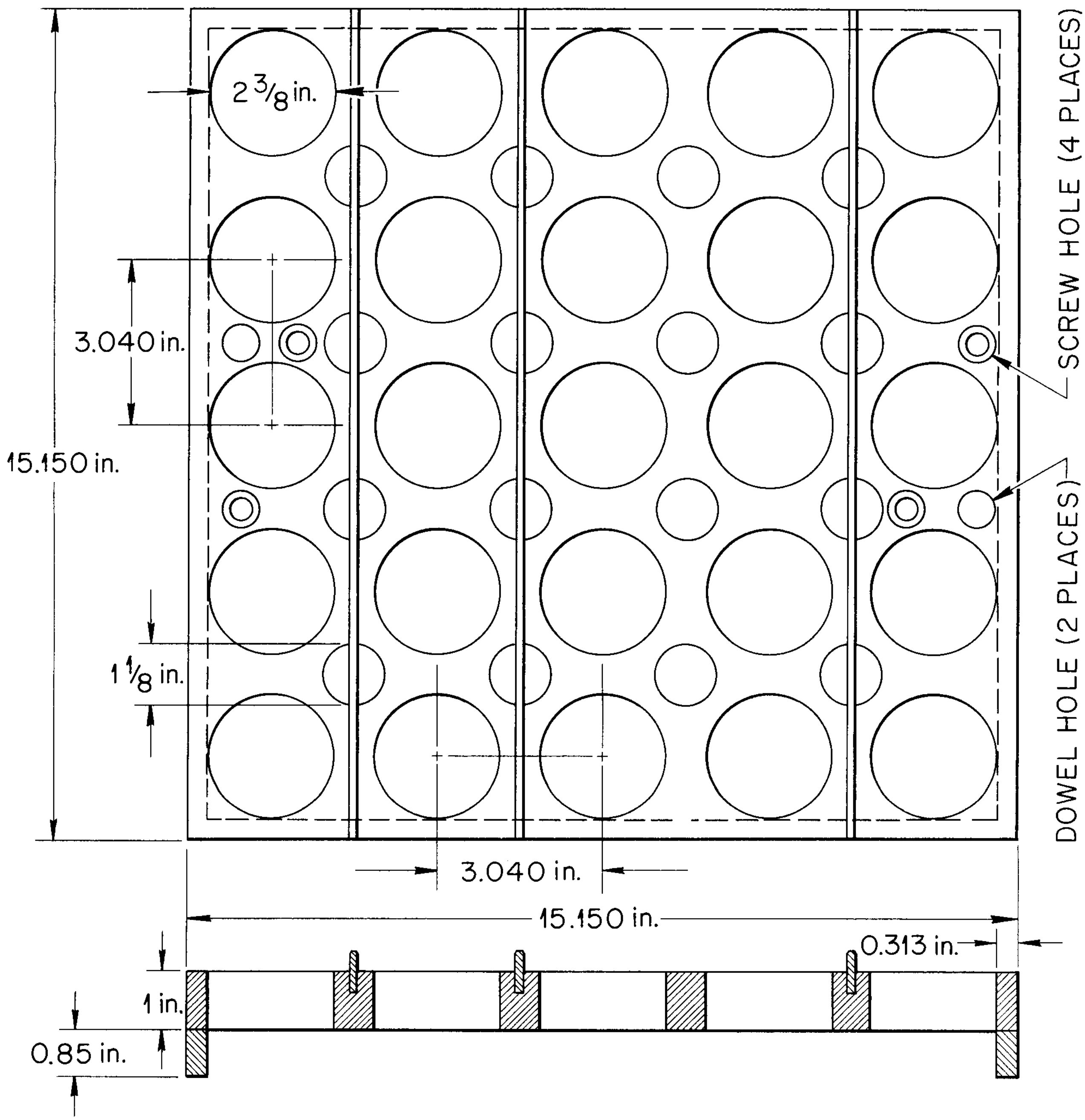

Fig. 1. Plan and Sectional View of Stainless Steel Grid Plate for BSR-II.

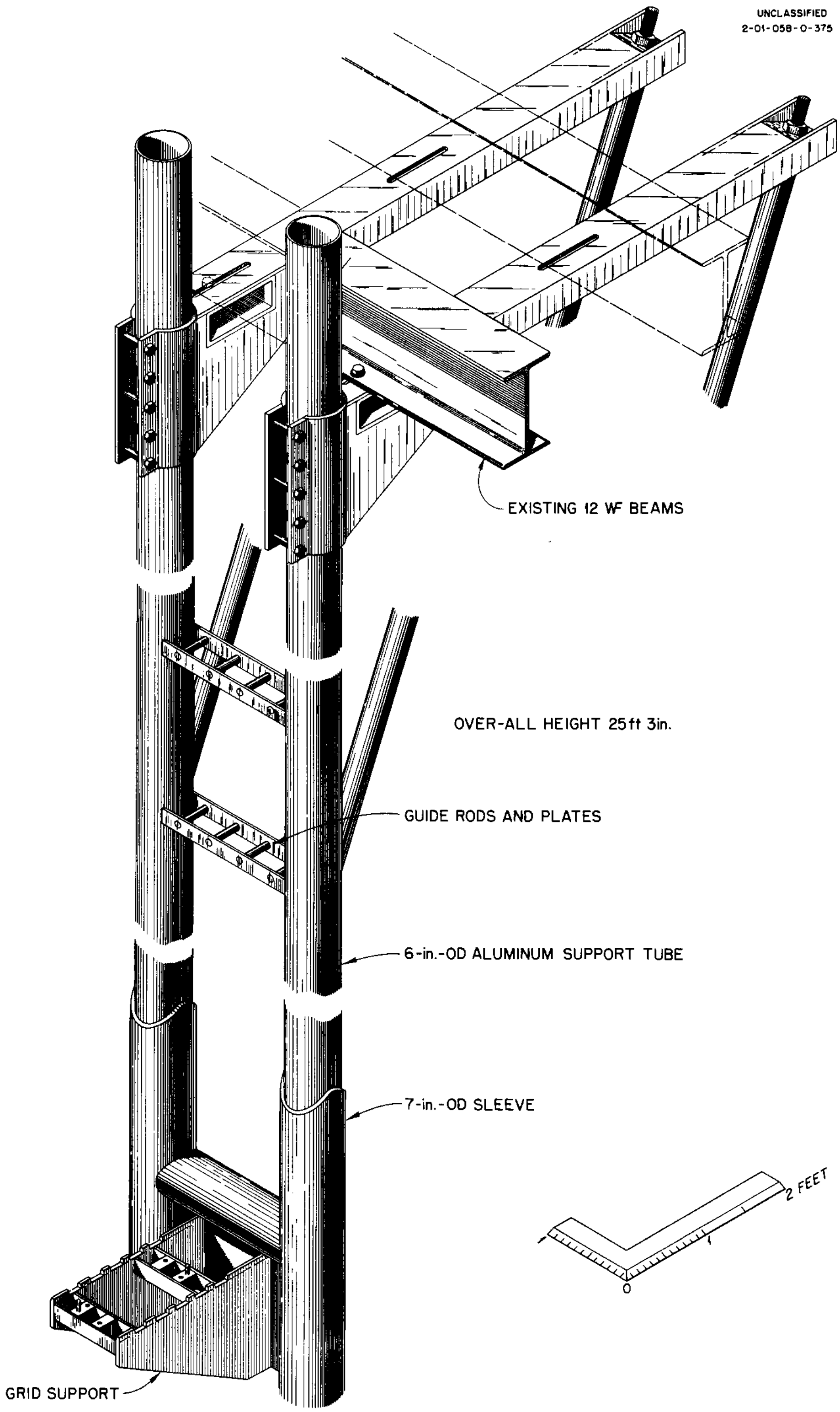

Fig. 2. View of Reactor Support Structure for the BSF. Both the BSR-I and the BSR-II grid plates will fit interchangeably over the two dowel pins, and will be secured with four screws.

cladding are type 347 stainless steel, 0.050 and 0.008 in. thick, respectively.

The total height of the fuel plates is 15.75 in., the height of the fuel-bearing region being 15 in. The over-all height of the elements is made as small as conveniently possible in accordance with the desire for compactness. The fuel elements have a bottom endbox welded to the side plates; this endbox supports the element in the grid plate and provides a passage for the water flow through the core. A small extension of the side plates above the core top provides room for the attachment of a cross member by means of which the element may be lifted and manipulated.

Figure 3 also shows a cross section of the fuel-bearing region of the special fuel elements that accommodate the control plates. There are to be four of these in the core. The outside dimensions are identical to those of the standard fuel element, and will be observed to be square. This permits the flexibility in location of the control plates referred to above. Note that the number of fuel plates in the control plate elements remains at 20, as does the number and width (0.120 in.) of the water spaces. However, the fuel plates have been narrowed in order to make room at either side of the elements for two control plates. These drop into channels formed by modifications of the side plates from flat plates into shallow troughs covered by a

UNCLASSIFIED
2-01-058-0-309

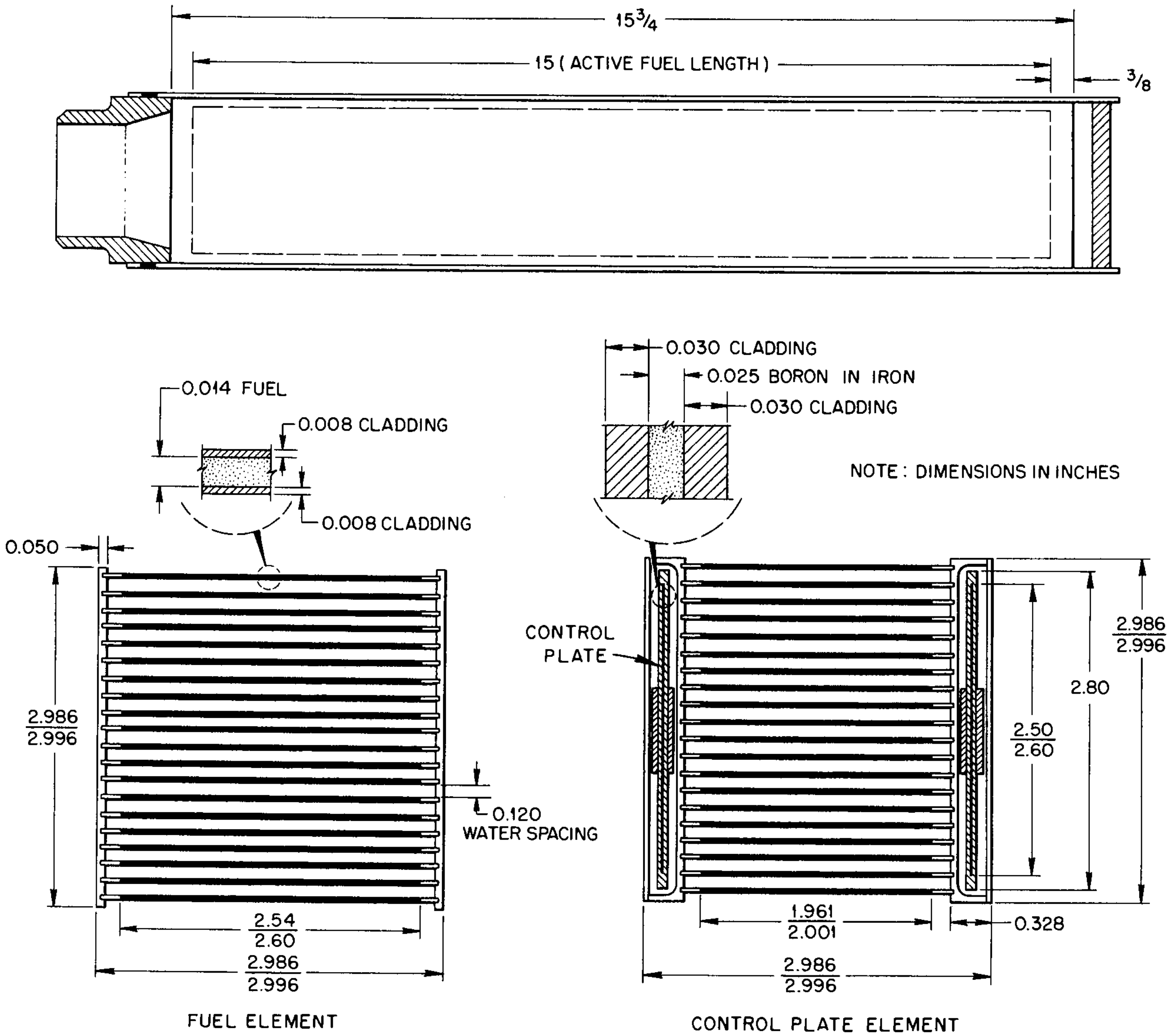

Fig. 3. Plan View of Fuel Element for BSR-II, and Cross Section Views of Fuel Element and Control Plate Element for BSR-II. The control plates are shown in place.

tackwelded 0.025 in. cover. The core portion of the control plates consists of a dispersion in iron of 4.5 g of boron enriched to 90% in B^{10}. The cladding is 0.030 in. of steel on either side; in addition, there are stiffening strips along the centerline which reduce deflections and are also intended to act as chafing strips if contact between control plate and channel sides does occur.

The pair of control plates for each control plate element is joined at the top by a yoke, so that each pair of plates moves together at all times. This yoke is attached to a control plate lift tube, at the top of which is an armature. The entire control rod manipulating mechanism is pictured in Figs. 4 and 5. It consists of a magnet, armature, accelerating spring and dashpot-and-piston decelerator. The entire assembly is enclosed in a 3-in.-dia. tube which is attached at the bottom to the control plate element, and which extends to the top of the support structure. All lift forces exerted by the drive system are exerted against this tube so that in no situation can a lifting force exist to lift the entire element out of the core. This outer tube is not shown in Figs. 4 and 5.

The effect of this arrangement is to drive the pair of control plates into the fully inserted position, when the magnet is de-energized, from whatever initial position the control plate occupies at the time of the drop. In order to re-engage the magnet and

UNCLASSIFIED
2-01-058-0-320

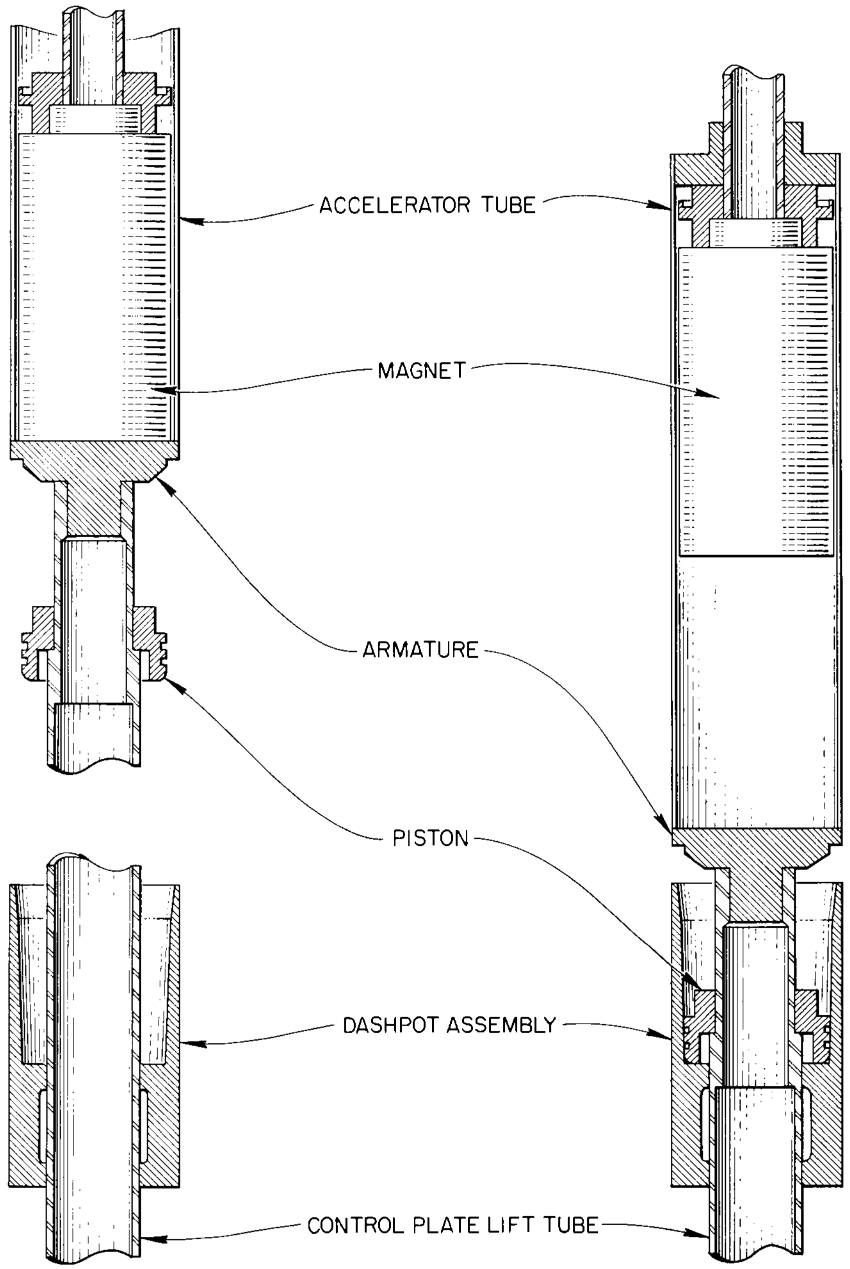

Fig. 4. Cross Section View of a Portion of the Control Mechanism in Withdrawn Position (l) and in Scrammed Position (r). The armature and piston are attached to the control plate lift tube, which slides through the dashpot assembly. The motion of the lift tube assembly is arrested by insertion of the piston into the dashpot. The control plate lift tube assembly is accelerated by the accelerator tube, which pushes down on the rim of the armature due to the spring pressing upon it from above (see Fig. 5). The assembly is held in the withdrawn position by the magnet when the magnet is energized and the armature is in contact with it. The magnet is supported by a lift tube which extends to the top of the reactor support structure and is positioned by the control rod drive motor there. An outer tube of 3 in. dia which supports the dashpot, and which is attached to the control plate fuel element below, and to the control rod drive mechanisms above is not shown.

UNCLASSIFIED
2-01-058-0-321

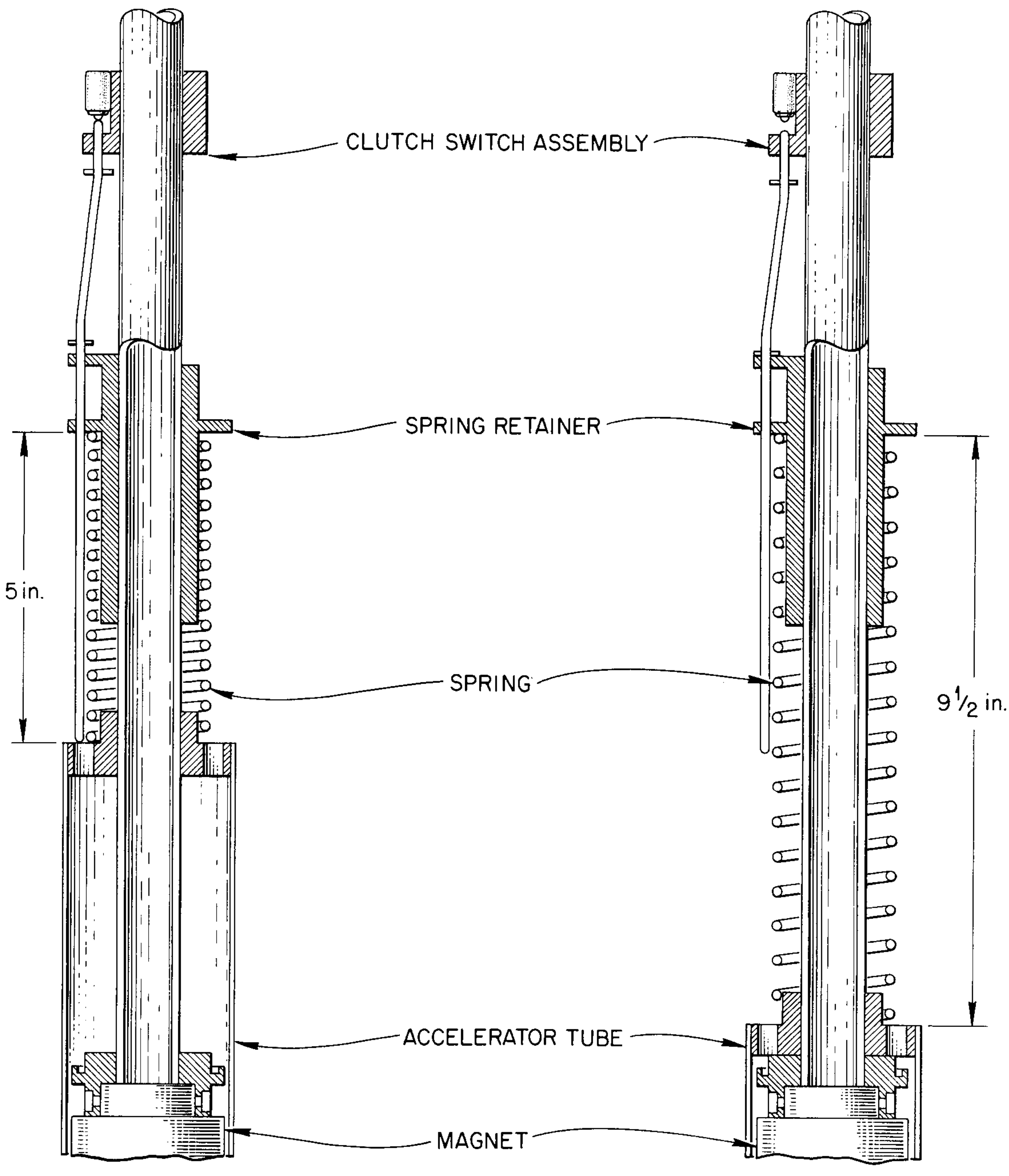

Fig. 5. Cross Section View of a Part of the BSR-II Control Mechanism. The accelerating spring is shown both cocked (l) and released (r). The spring retainer is firmly attached to the magnet lift tube, as is the magnet. The accelerator tube fits loosely over the magnet, and over the magnet lift tube, so that it is free to slide downward under the force of the spring, pushing against the armature below the magnet (Fig. 4). The clutch switch assembly signals whether the armature is against the magnet or not. An outer tube of 3 in. dia which is connected to the control rod drive motor assembly above, and to the control plate assembly below is not shown.

armature after a scram it is necessary to drive the magnet all the way down to contact the armature. In this process the spring is necessarily cocked, since during the lowest part of the travel of the magnet lifting tube the accelerator tube bears against the armature, forcing the spring to compress. Thus it is never possible to pull the control plates from the fully inserted position without having cocked the accelerator spring. Since there is no mechanical latch or other impediment to the dropping of the control plates it is assured that the control plates will insert whenever the magnet current drops below the holding current. At the bottom of its travel the entire moving system of control plates, yoke, lift tube, armature and accelerator tube is brought to a stop by a decelerator "dashpot assembly" into which a piston attached to the lift tube fits. The decelerator has been designed and tested to yield a maximum velocity of 1 in./sec. at the moment of the bottoming of the piston in the decelerator, which forms the stop.

The design of this decelerator is described in Appendix 1. The performance of the control system will be described in detail in the section on reactor kinetics.

II. NUCLEAR CALCULATIONS

The critical mass and neutron flux calculations for the BSR-II were carried out by means of the 30-group multiregion "Eyewash" code on a UNIVAC computer. The details of these calculations will be found in Appendix 2.

These calculations were carried out in order (1) to determine the feasibility of achieving criticality within the limitations of size desired, and also within the bounds of the possible from the metallurgical and fabrication point of view, (2) to determine the optimum dimensions and configuration of the fuel and cladding regions, (3) to help determine the design of the control devices, (4) to predict the neutron energy and flux shape distributions so that good heat transfer calculations could be made, (5) to determine the neutron lifetimes in order to assess the reactor kinetics situation, and (6) to predict the temperature coefficient of the reactor.

The results shown in Fig. 6 are from a calculation assuming a cladding thickness of 0.005 in. It must be borne in mind, however, that as a result of the calculations a cladding thickness of 0.008 in. was adopted for the final design. Nevertheless, the nuclear calculations remain valid, since the increase in cladding thickness is accompanied by a corresponding reduction in "meat" (fuel region) thickness so that the

UNCLASSIFIED
2—01—058—0—310

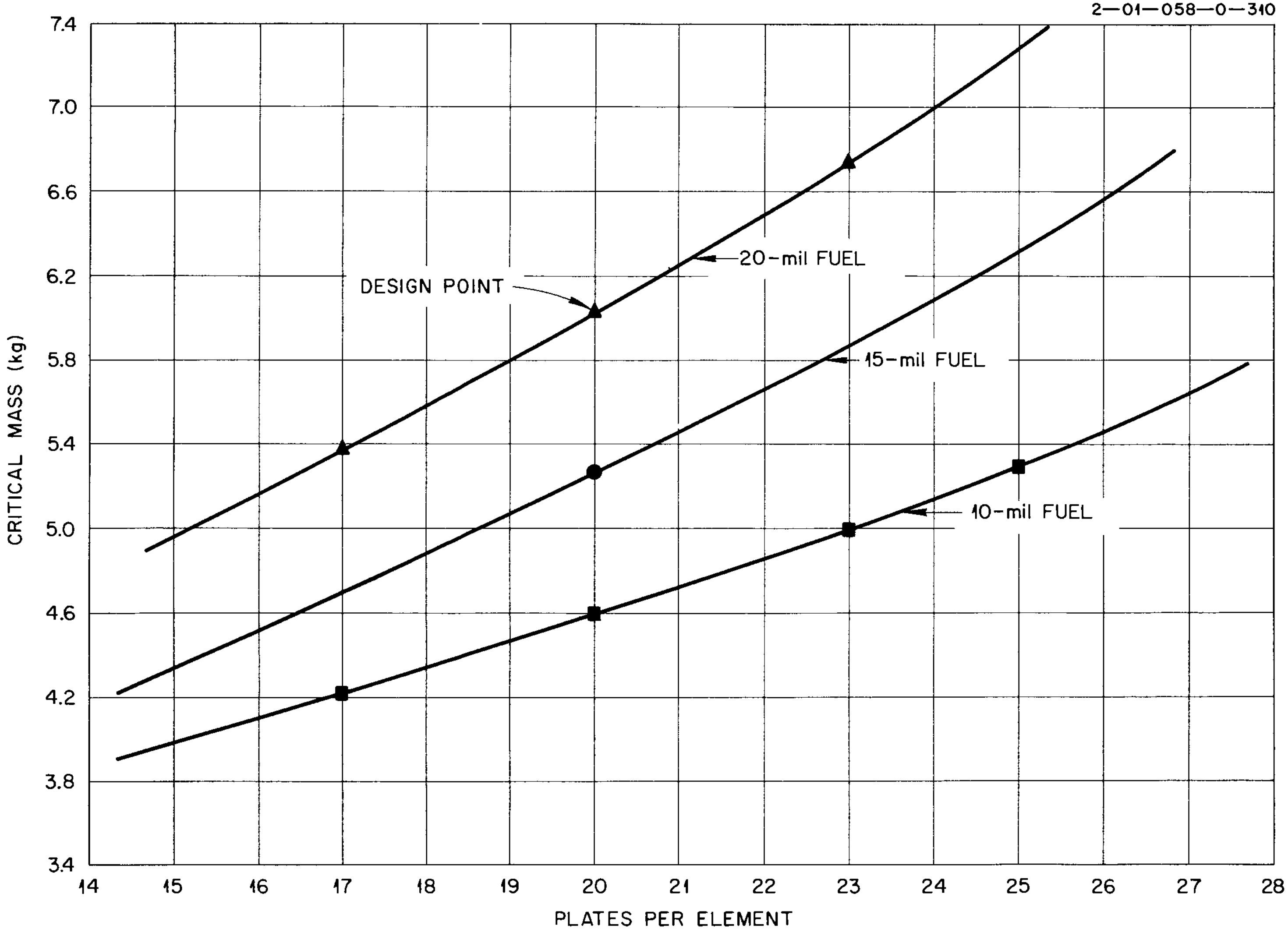

Fig. 6. Calculated Critical Mass as a Function of the Number of Fuel Plates per Element for Three Different Fuel Region Thicknesses in BSR-II. The points represent the results of calculations with the UNIVAC "Eyewash" code. The lines are interpolations between the calculated points. The calculation with 20 mil fuel region thickness and 5 mil clad is equivalent to the final design dimensions of 14 mil fuel region and 8 mil clad.

total quantities of steel and uranium remain unchanged. In each case the amount of fuel needed for a cold, clean, critical reactor is obtained from a series of calculations wherein the amount of uranium is varied. Figure 7 shows the results of these calculations for some few cases. From these primary curves the effect of change in fuel content on reactivity can be derived.

It is evident from Fig. 6 that the amount of fuel required for criticality depends on the number of fuel plates per element. This is expected because the introduction of additional fuel plates introduces more stainless steel in the form of cladding and fuel cermet and reduces the water volume fraction in the core. Similarly, the thickness of the fuel region affects the critical mass because, for the same fuel content per plate, the steel content increases with thickness, and the water content is diminished. The choice of the design point at a calculated fuel region thickness of 0.020 in. was dictated by structural considerations, which called for a minimum plate thickness of 0.030 in. in order to assure adequate stability against warping or mechanical damage to the plate. The number of fuel plates determines the maximum power of the reactor since the limiting factor is the heat transfer rate from plates to water. The limit is attained when local surface boiling occurs at the hottest plate surface point of the core. Therefore the maximum permissible power level is directly proportional to the heat transfer surface,

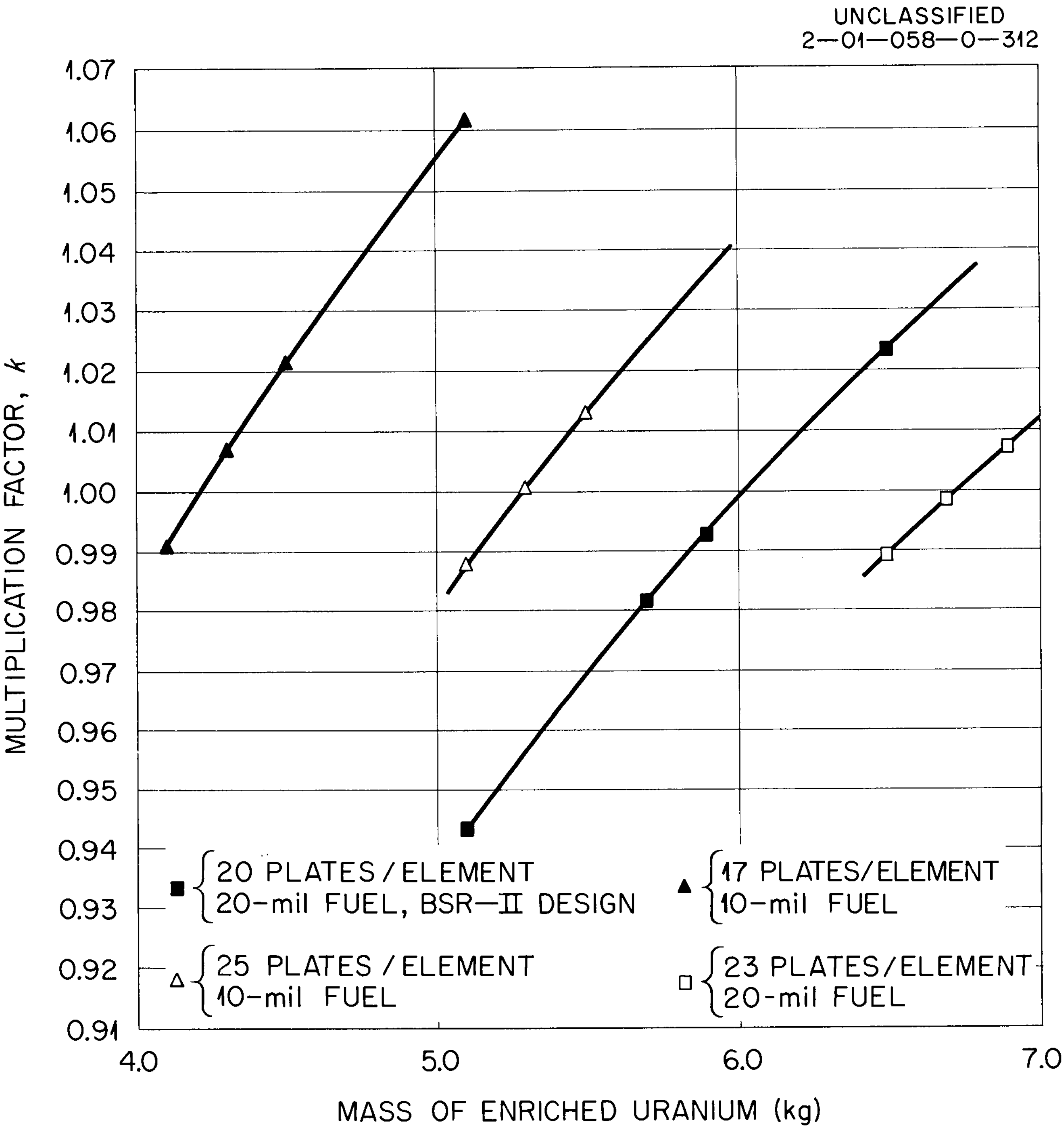

Fig. 7. Multiplication Factor, k, as a Function of Amount of Uranium for Several Possible Design Choices for BSR-II. The points represent individual "Eyewash" calculations, with interpolations in the form of the solid lines. The design case is represented by the solid black squares.

which in turn is directly proportional to the number of fuel plates, all other factors remaining equal. Twenty plates per element was taken to be a suitable compromise between fuel economy and heat transfer capacity.

The cold clean, critical mass was calculated to be 6.03 kg. However, the amount of fuel available in the core must be sufficient to allow for enough excess reactivity to operate, as well as for the uncertainties in the calculation. There must also be enough flexibility to permit operation if the calculated critical mass proves to be an overestimate. Therefore the inventory shown in Table 1 is proposed. This 35-element inventory permits full (25-element) loadings of as much as 6986 g, and as low as 5041 g, ($\pm$16% in mass), which should be a sufficient range for the contingencies foreseen at the present time.

The fuel content of a single plate is 14.5 g of uranium, which, with a fuel region thickness of 0.020 in. would lead to a fuel concentration of 16.8 wt% UO_2 in the fuel material. Since a concentration of 25 wt% is feasible, it would be possible to reduce the fuel region thickness. However a mimimum thickness of 0.030 in. for the entire plate is necessary for structural integrity as discussed above, so the fuel region reduction cannot be used to reduce the total steel content, and thus the critical mass. However, the fuel region can be made thinner, and the cladding thickness increased correspondingly, thus achieving a greater cladding thickness at no expense in increased

Table 1. Proposed Fuel Inventory of BSR-II

Type of Element	Number	U Content/Element (g)	Total U in Elements of That Type (g)
Full elements	21	290	6090
Half elements	4	130.5	522
Quarter elements	6	72.5	435
Control elements	4	224	896
Total	35		7943

steel content. The design therefore calls for a fuel plate cladding thickness of 0.008 in. and a total plate thickness of 0.030 in. which leaves a fuel region 0.014 in. thick. The fuel will then contain 1.83 g of UO_2 per cubic centimeter of fuel material, which amounts to a concentration of 23.6 wt % of UO_2.

The temperature coefficient of the reactor has been calculated by means of the "Eyewash" code as follows: The thermal group was taken at the lower end of fast group 30 in most cases, corresponding to a temperature of 66°F. A calculation was also carried out using 29 fast groups, with the thermal group at the lower end of the 29th fast group. This corresponds to a temperature of 183°F. The density of the water in the core was adjusted for the thermal expansion from 66 to 183°F. The temperature coefficient so calculated was found to be about $-(2 \times 10^{-6})/°C$. The negative value of the temperature coefficient is chiefly due to the decreasing water density with increasing temperature, which causes increased neutron leakage.

III. HEAT TRANSFER CALCULATIONS

Heat transfer calculations were carried out to determine the maximum power level attainable with the reactor as designed. The limitation on power is assumed to be the attainment of a temperature sufficient to cause local boiling at the hottest surface point in the reactor. The calculation is described in Appendix 3. The result indicates that with 20 plates per fuel element the boiling point would be reached at a power of almost exactly 1000 kw. It is therefore proposed to set a power limit of 750 kw for initial reactor operation. It is anticipated that experimental measurement of the temperatures in the fuel plates will be made before the designed maximum power is attained. The method used will be similar to the method used for such a measurement made on the BSR-I.[4]

IV. REACTOR CONTROL AND SAFETY

The control of the reactor is achieved by means of eight plates of steel containing 4.5 g each of boron enriched to 90% in B^{10}. As previously described, the plates will be attached in four pairs to the control rod drive mechanisms. The considerations of reactor control are concerned with (1) determination of the total value of the eight control plates in terms of reactivity content, and (2) a consideration of the kinetic behavior of the control system, and of the reactor system as a whole.

The first part of this calculation is based on a measurement of the value of an equivalent control plate in the center position of the BSR-I. As shown in Appendix 4, this value is 3.30% $\Delta k/k$.

Since the plates occur in pairs at a separation distance of about 6.5 cm, an experiment was also carried out to determine the interaction of two plates at such a separation. This measurement is also described in Appendix 4. The results show that there is no important shadowing of the two plates. The total worth of eight plates in the BSR-II is thus obtained from the worth of a single plate in the BSR-I multiplied by eight, and also multiplied by factors to include the difference of the worth of a control plate in the BSR-II as against the BSR-I, and to allow for the fact that not all plates can be located at the center of the core. The former of these two factors is arrived at by a consideration of the control rods in the APPR-I and in the MTR. These two reactors have core compositions similar to the BSR-II and BSR-I, respectively, and the control rods in the two cases are very much alike. Experiments with these two reactors show that the worth of a single control rod in the APPR-I is about half that in the MTR. It is assumed that this value also holds for the BSR-II and BSR-I. The second factor, concerning the placing of the control plates, is very much dependent on the choice made from the many possible configurations of the control plates. It is therefore one of the aims of the experimental program to be carried out with this reactor to examine this dependence in detail. However, it is possible to achieve a configuration wherein all eight plates are located in the inner three by three element region, with their centers less than halfway out to the edge of the core.

The calculated flux shape curve shown in Fig. 8 was used to estimate the effectiveness of the plates in such a configuration, assuming the value to be proportional to the square of the unperturbed flux at the location of the plate, and assuming no interaction between plates. With this assumption the result is a worth of 0.6 times the central rod worth. However, owing to the flux shape alteration imposed by the presence of control plates, the value of other control plates

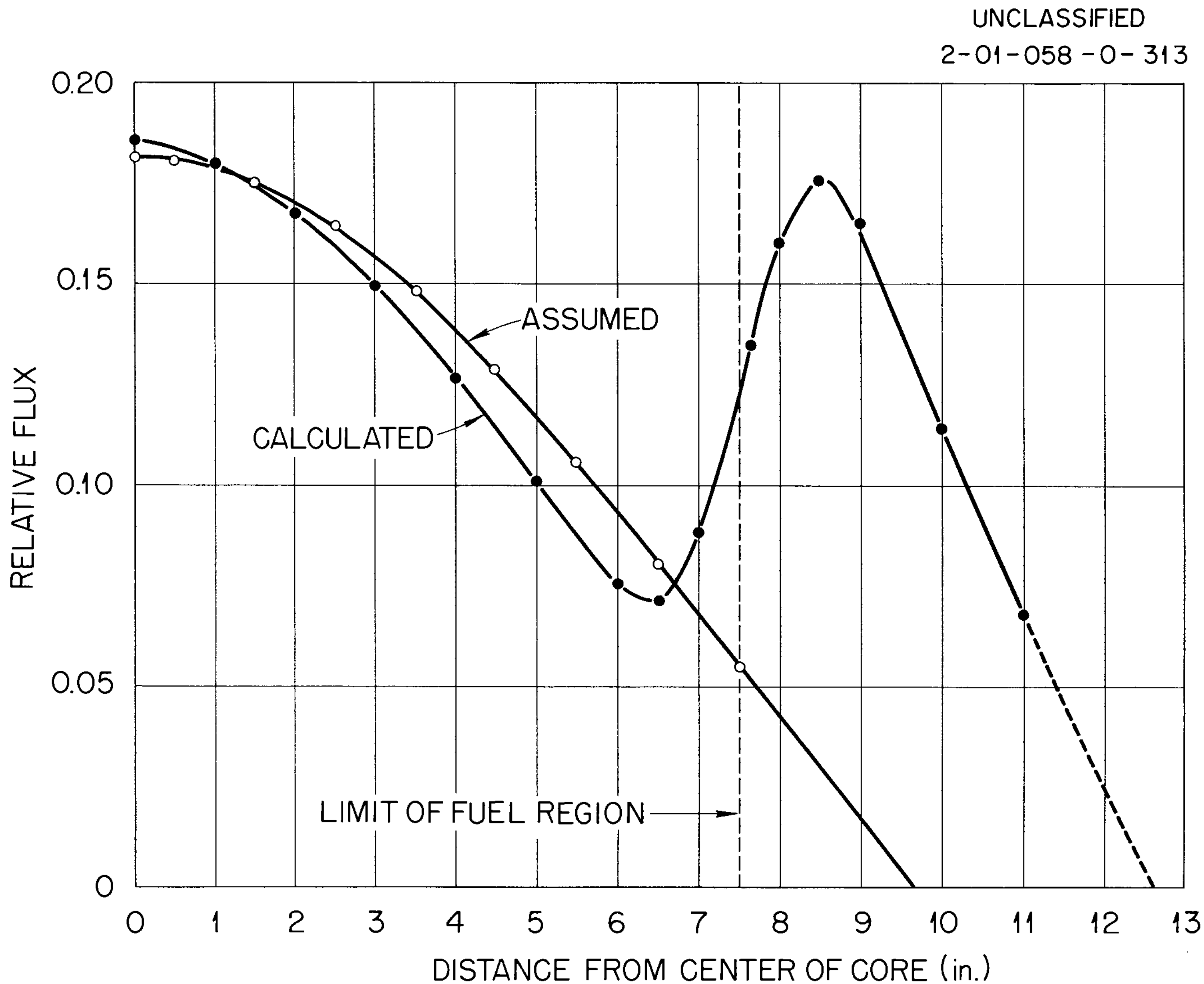

Fig. 8. Comparison of the Shape of the Thermal Flux in BSR-II, as Calculated by the "Eyewash" Code, with a Curve Consisting of the Center Portion of a Cosine Curve. The portion of the cosine curve used is so chosen as to yield the same volume-weighted peak-to-average ratio as the curve calculated by "Eyewash." The cosine curve is used in the heat transfer calculation on BSR-II.

would be enhanced somewhat. This is apparent when one considers that a flux depression in one location due to a control plate must increase the relative flux elsewhere. So a value of 0.5 to 0.75 for the geometric factor may be taken as reasonable. Applying these conversion factors to the experimental results gives a predicted total rod worth of 6.0% to 10.0%.

It is anticipated that certain configurations of the control plates, for example, configurations in which the control plates surround the central fuel element completely or divide the core into two separate regions, may increase the total value above the figures quoted, but it will become apparent from the kinetic considerations that the mimimum figure of 6% is adequate. Experimental measurements of the actual worth of the control plates will be carried out with the BSR-II when it is operating.

In order to consider the kinetic behavior of the control system, a series of experiments was carried out in which the time response of a mechanical mockup of the control system was investigated. These experiments are described in Appendix 5. The results are shown as a series of curves in Fig. 9, which give the position of the leading edge of the control plate as a function of time after the scram signal for various conditions. The design calls for a 66-lb spring, which was one of those that were tested. This result is combined with a measured rod position vs. reactivity curve obtained for the BSR-I.

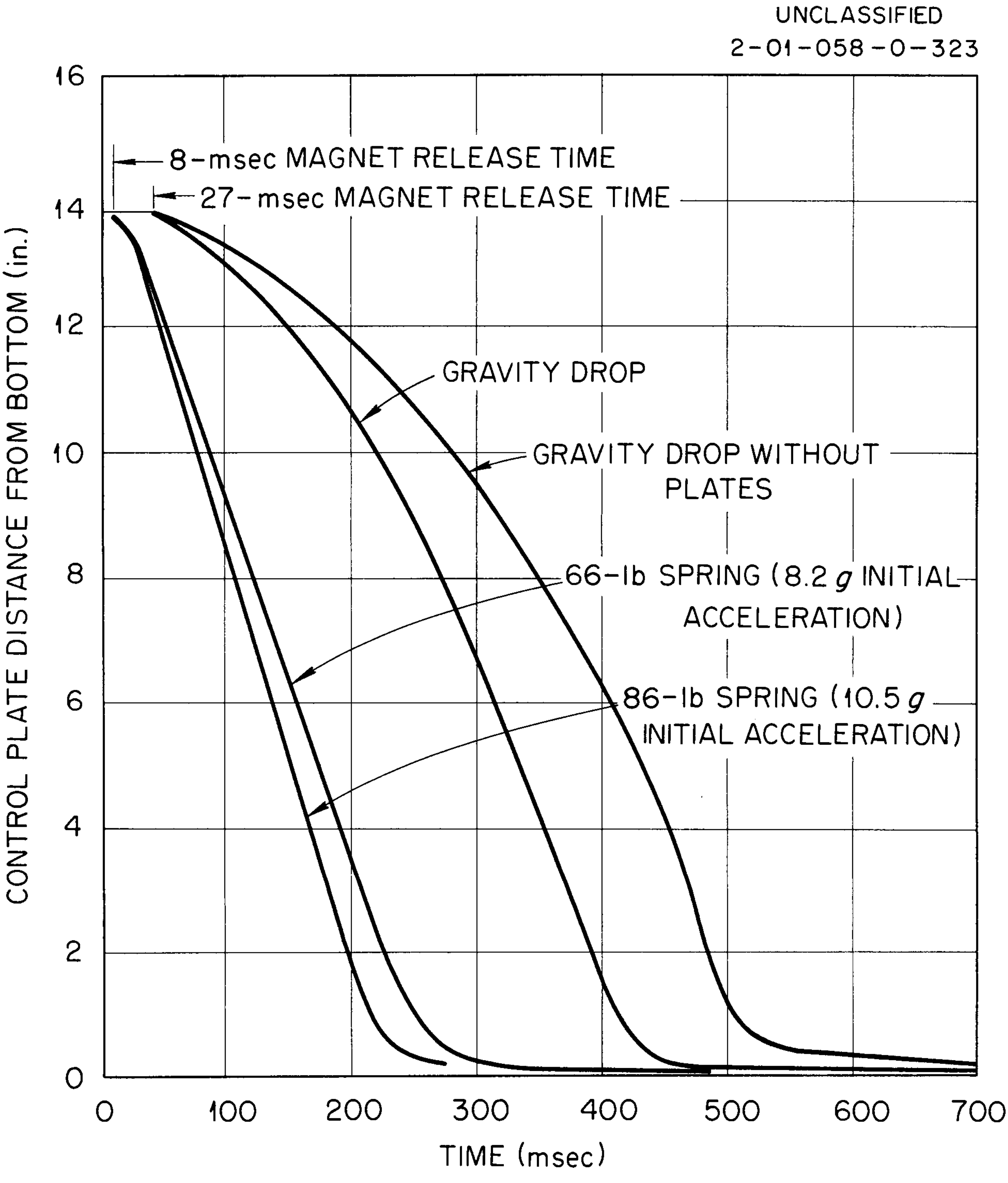

Fig. 9. Results of an Experimental Test of the Control Plate Drop Mechanism of the BSR-II. The position of the lower edge of the control plate is shown as a function of time after initiation of the scram signal. The 66 lb spring curve corresponds to the design selected for BSR-II.

It is assumed that in the BSR-II the shape of the curve will be the same, as normalized over the 15-in. core height. This latter assumption is conservative, since the higher poison content of the BSR-II leads to a flatter core flux than is found in BSR-I, thus increasing the initial effectiveness of the rod insertion somewhat. The result, in terms of fraction of total rod worth inserted as a function of time, for various initial insertions, is given in Fig. 10 for the design spring. It is to be observed that the initial slope, as well as the initial value, is dependent on the preinsertion distance. In order to take advantage of this factor, the control system is so designed as to permit withdrawal only to within 1 in. of the top of the core. This 1 in. preinsertion is designed to improve the time response of the system if a scram signal occurs when the rods are all fully withdrawn.

The time response of the control system was used as input to an analog computation described in Appendix 6 which was carried out to determine the reactor behavior using the designed control system. The calculated neutron generation time for the reactor is 26 μsec for prompt neutrons. This number is based on a calculated thermal-neutron lifetime of 20.1 μsec, and an assumed slowing down time of 10 μsec, with 19% of the fissions being in the epithermal group. Since, as pointed out in Appendix 2, the epithermal fissions are mostly in the lower epithermal

UNCLASSIFIED
2-01-058-0-325

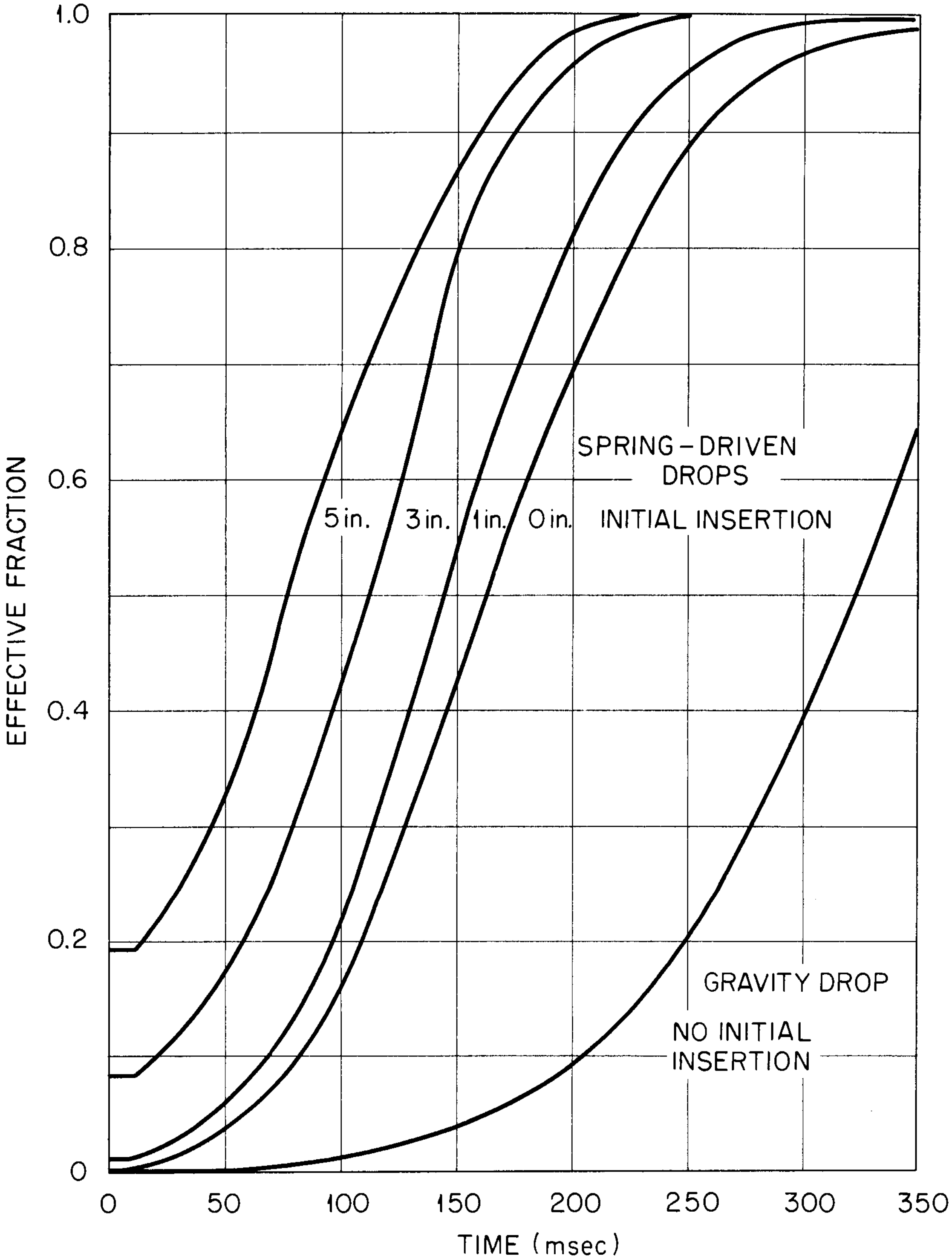

Fig. 10. Fraction of Total Control Plate Worth Inserted as a Function of Time After Initiation of Scram. The acceleration was accomplished with the 66 lb spring designed for BSR-II, and various initial insertions are considered. For comparison a similar curve for gravity dropped control plates is also shown.

range, it was assumed that the fast fissions would be initiated 10 μsec after the birth of the initiating neutron. It was thus assumed that neutrons causing fast fission nevertheless live the full slowing down time, though none of the thermal diffusion time, between birth and capture. This generation time is for prompt neutrons only. The calculated 26-μsec generation time is conservative, i.e., too short, since a portion of the neutrons will spend part of their lives in the water reflector, where the lifetimes are much larger. Therefore, the effective generation time is larger than the 25 μsec used as a basis for the analog calculation.

In the analog computations the criterion for a safe reactor control system was taken to be that the reactor power must not surge to a level greater than 1000 times the level at which the scram signed was initiated. This factor of 1000, used as criterion because it is the largest factor the analog computer is able to handle, is conservatively low from the reactor damage viewpoint. This becomes apparent from an examination of data obtained with the SPERT-I reactor.[20] With this reactor experiments were carried out in which self-limiting excursions were initiated in the initially subcooled ($\approx 25^{\circ}C$) reactor. The fuel plate surface temperature at the center of the reactor was measured during each excursion. In the BSR-II the maximum excursion possible (consistent with the peak operating power of 750 kw and maximum flux increase factor of 1000) is 750 Mw. The maximum fuel plate surface temperature recorded for a SPERT-I excursion of this magnitude was $200^{\circ}C$. This temperature is far below the melting point of stainless steel (1400°C). The temperature increases in these two reactors are at least somewhat comparable since the higher power density per watt of reactor power in the BSR-II is largely offset by the smaller energy liberation in an excursion of a given magnitude due to the shorter neutron generation time in the BSR-II.

Accordingly, the positive period that will yield an excursion of a factor of 1000 is determined for each condition of interest. The period vs. reactivity curve for a neutron generation time of 25 μsec then also permits the determination of the excess reactivity corresponding to such a period (Fig. 11). Table 5 in Appendix 6 shows the result of this calculation.

Under the design conditions of a total plate worth of about 8%, with a neutron generation time of 25 μsec, and using the drop test data for the 66-lb drive springs, there results a minimum period of 6.0 milliseconds that can be reversed within the factor of 1000 in flux rise set up as criterion.

It is interesting to observe the effect that the total rod worth has on the minimum period that is capable of being controlled. In Fig. 12 is shown a plot of both the period and the excess reactivity that can be controlled, as a function of total rod worth. It is to be observed that the amount of excess reactivity does not depend strongly on the total rod worth.

UNCLASSIFIED
2-01-058-0-328

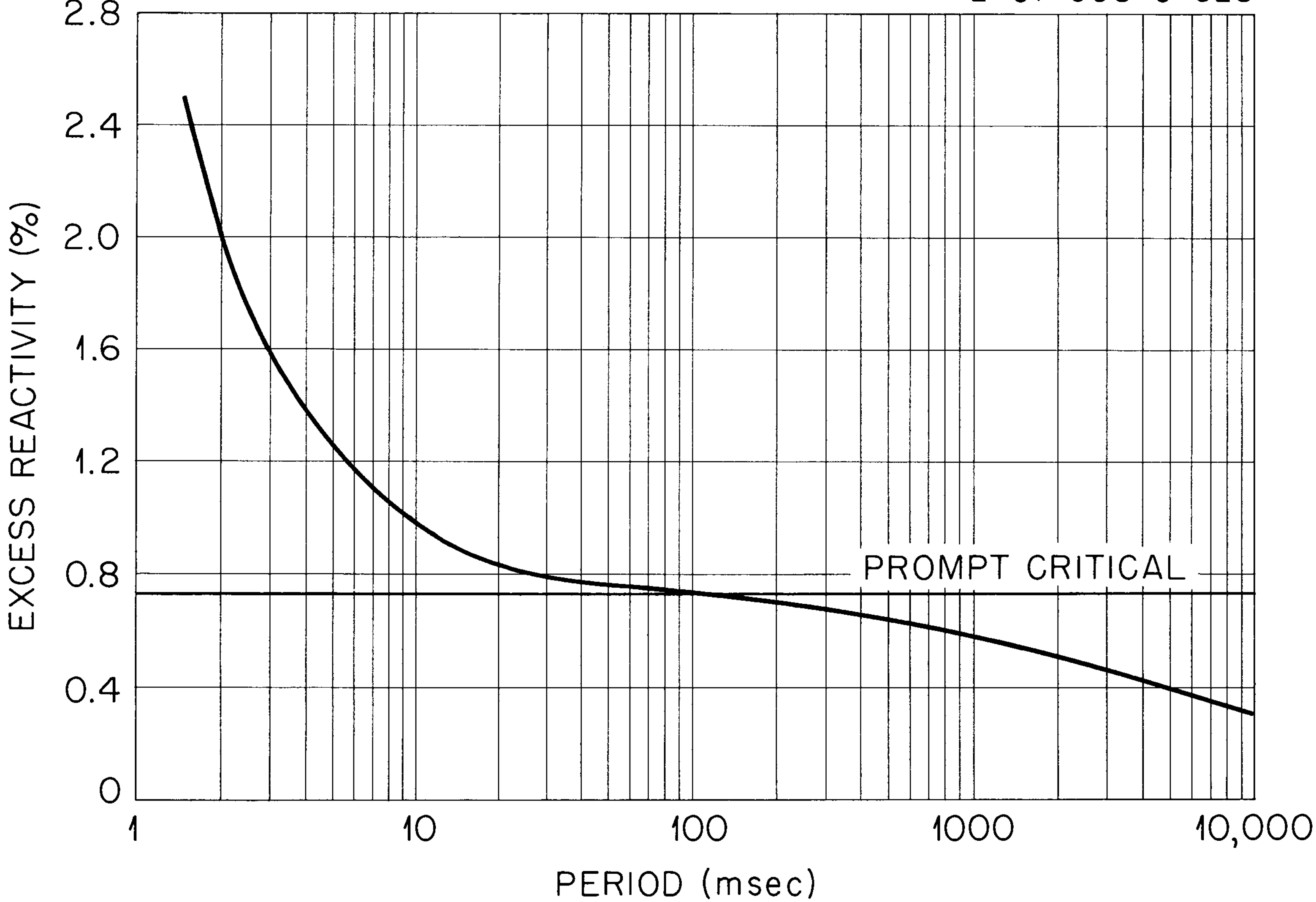

Fig. 11. Reactor Period as a Function of Reactivity for a 26 μsec Prompt Neutron Generation Time. This generation time is the one calculated for BSR-II, neglecting the effect of the longer lifetime of neutrons in the H_2O reflector.

UNCLASSIFIED
2-01-058-0-327

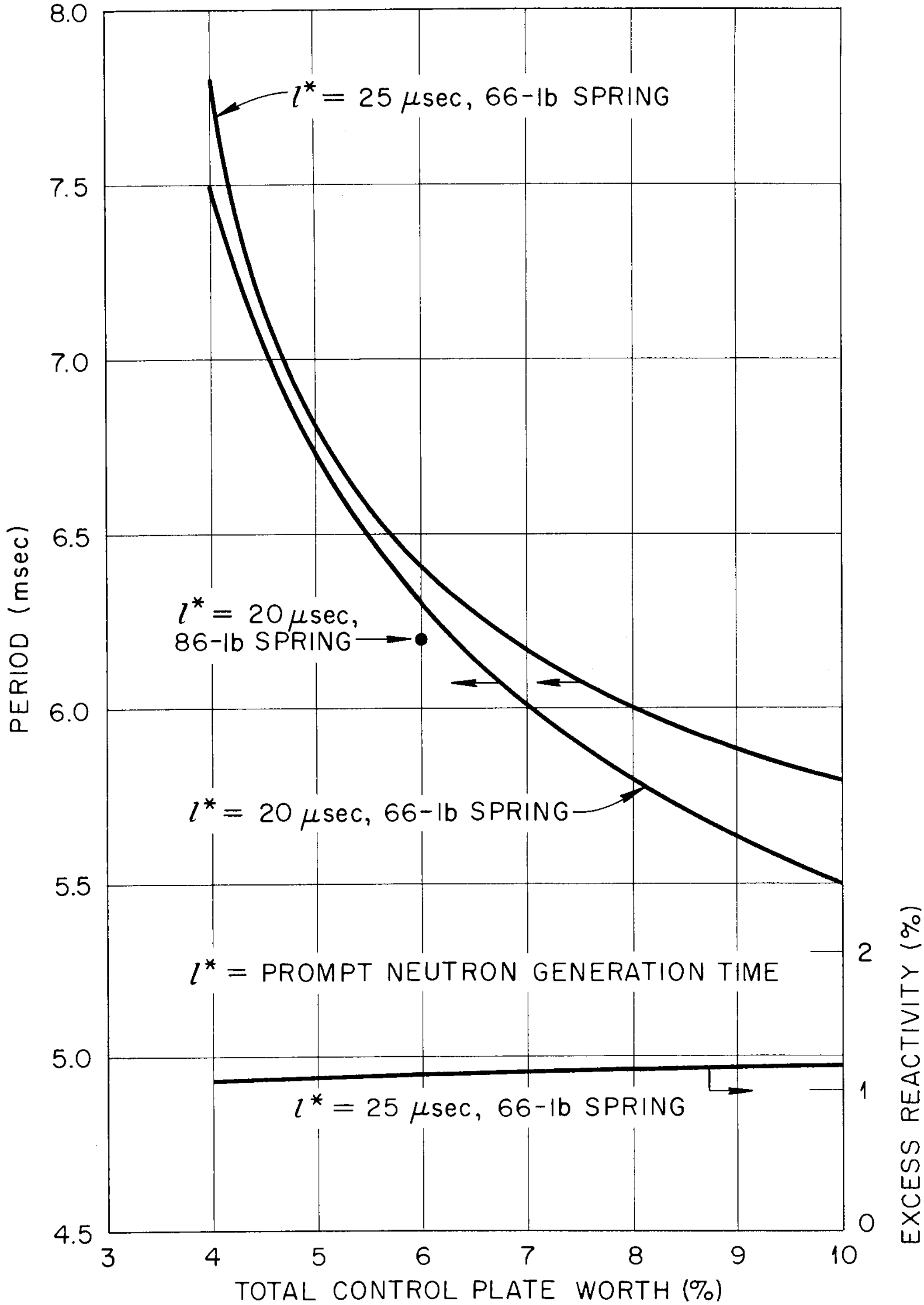

Fig. 12. Period and Per Cent Reactivity that can be Reversed Within a Three Decade Power Excursion as a Function of Total Control Plate Worth in BSR-II. This is the result of an analog calculation. The curve labelled "$1^* = 25\ \mu$sec, 66 lb Spring" corresponds to the design conditions of the BSR-II.

This can be interpreted to mean that in the case of a scram the failure of one of the four control plate pairs to drop would not be serious, since the excess that can be controlled by the action of all rods is only very little more than that which can be controlled by three-fourths of the total rod worth. A more realistic way to consider this aspect of the reactor behavior is to realize that in no case can a very large excess above prompt criticality be controlled, so that it becomes imperative to remain at all times in a condition such as to preclude a step insertion of more than about 1.0% of excess reactivity.

It is to be remembered that the calculation assumes a true step increase in reactivity, one occurring in zero time. Any physical event leading to an increase in reactivity, such as dropping fuel into the core, would lead instead to an increase in reactivity with time (a ramp), which would be much more readily controlled than a step increase. The implications of these calculations for operation of the BSR-II will be discussed below.

It is conceivable that an earthquake, or any other major shock might rupture the BSF pool and release the water, thus removing the coolant, and simultaneously shutting down the reactor. In such a case the after-heat would be removed by conduction along the structure, convection to the air, and radiation. The temperature rise in the core due to such a situation was estimated from an experiment done with the BSR-I, as discussed in Appendix 7. The temperature will not rise high enough to cause melting and release of fission products.

V. MECHANICAL STRESS INTEGRITY

Calculations have been carried out to determine the mechanical strength of the fuel elements and control plate elements of the BSR-II. The following problem was considered: What force, exerted laterally against the top of a fuel or control plate element, will stress the element to the yield point at the point of greatest stress? This greatest stress, under the force considered, lies at the lower end of the plate section of the fuel and control plate elements. For this calculation the element was considered to be standing free in the grid plate with no support from the adjacent elements. The latter assumption would be true under the conditions of largest separations between elements consistent with the design tolerances. In the calculation for the control plate elements no allowance was made for the additional strength due to the 3-in.-OD magnet guide tube, which extends from the element to the control plate drive motor at the top of the support structure. The results are shown in Table 2.

Another calculation was performed to determine the strength of the welds holding the plate section of each fuel element and control plate element to the lower end box. It was found that a stress sufficient to cause yielding of the plates, as described above, will not cause failure of the welds.

Table 2. Force Applied Laterally at Top of BSR-II Fuel and Control Plate Elements Which Will Cause the Elements to Yield at the Lower End Box

	Force Applied Parallel to Fuel Plates (lb)	Force Applied Perpendicular to Fuel Plates (lb)
Standard Fuel Element	820	284
Control Plate Fuel Element	1030	529

Table 3. Force Against Control Plate Channel Cover Required to Cause Binding of Control Plate If Applied at Center Point or Along Center Line of the Cover Plate

	Force Applied at One Point (lb)	Force Applied Along Centerline (lb)
Simply Supported	14	54
Rigidly Clamped	53	210

Consideration was also given to the possibility that a lateral force against the top of the control plate element might cause a deformation sufficient to bind the control plate, even though not of sufficient severity to cause permanent damage to the element. A calculation indicated that a force of 995 lb applied laterally against the top of the control plate element in a direction parallel to the fuel plates would cause binding of the control plate under the conditions of the minimum clearances permitted by the design tolerances. This is a force of almost the same magnitude as the force required to cause yielding. A force applied to the 25-mil-thick cover of the control plate channel may deform this plate to the extent that it would cause the control plate to bind, thus preventing its free motion. The magnitude of the force needed to accomplish this was computed under two assumptions. In one case the plate is assumed to be simply supported by the tack welds that hold it to the control plate element side members. In the other the plate is assumed to be rigidly clamped by these welds. The physical situation lies somewhere between these two assumed cases, since the plate is held against rotation by the welds, but the member holding the plate is not so rigid as to constitute a truly rigid clamp. Under the influence of a force applied to the cover plate, the U-shaped member would be deformed somewhat to accommodate the motion of the cover plate.

The calculation was made both for a force concentrated on a single point (the center of the cover plate) and for a force uniformly distributed along the vertical centerline of the cover plate. The results are shown in Table 3. In all these cases it was assumed that the deformation required to cause binding is the minimum possible in view of the design dimension tolerances. This is 0.046 in. The average clearance is 0.059 in. The details of these calculations are to be found in Appendix 8.

The force needed to cause yielding of the BSR-I fuel elements is about 60% of that calculated for the BSR-II. Since no mechanical deformation of the BSR-I fuel elements has been experienced during several years of operation, the greater strength of the BSR-II elements should assure safe operation in this respect.

The relatively small forces needed to cause binding of the control plates in the cases where the force is supplied in localized fashion directly against the cover plate serve to emphasize the need for caution where control plates are loaded at the core edge. However, in such a location the nuclear worth of the control plates is very low so that, in a given configuration, not all of the four pairs of plates would be placed in such a vulnerable position. In addition, it is a procedural practice that change of location of large equipment in the vicinity of the reactor, and all moving of the reactor itself, will be undertaken only with the reactor in the shutdown condition. The primary purpose of the cover plates on the control plate channels is to prevent any accidental lifting of the fuel element adjacent to the control plate during control plate withdrawal.

VI. OPERATING PROCEDURE

Since the new reactor will utilize the present well-tested BSR control system up to the magnets, it is proposed that operation of the BSR-II be carried out in accordance with the procedures outlined in ORNL-2448, "Operating Procedure for the Bulk Shielding Reactor, Fourth Edition," which will be available about Aug. 1, 1958, and which replaces ORNL-2018, "Operating Procedure for the Bulk Shielding Reactor, Third Edition."

The procedures outlined in this report represent a tested and working method of assuring correct function of the safety circuits prior to and during operation, and also specify the safety precautions to be observed in loading and operating the reactors. The approach to criticality with an unfamiliar loading is to be carried out in the manner specified, that is, by a careful and frequent use of the subcritical multiplication procedure to determine how close to criticality any given configuration is.

Prior to such a loading all four control plate systems will be installed and tested and will be functioning. During the initial loadings it is proposed that the procedure described in Section II ("Test Scram Circuits") of Appendix B of ORNL-2448 be carried out after loading each five or six elements, or more frequently at the discretion of the reactor supervisor.

The Operating Procedure provides that the loading of the BSR-II be carried out in such a manner as to have present at all times a core of such configuration as to minimize the effect of adding an additional element to the existing configuration. This means that there will be no loading of a configuration such as to leave a hole or gap in the core into which a fuel element might be accidentally inserted to cause a large reactivity effect. It also provides that, in the event an interior fuel element is to be removed or exchanged, the outer fuel elements be removed before doing so in order that no dangerous void exists at any time in the core. In the absence of voids or notches in the core configuration, the maximum increase in reactivity occasioned by a single fuel element dropped onto the top of the core, or placed next to it, is measured to be of the order of 0.6% as determined in a BSR-I experiment in which a single full fuel element was placed next to a compact critical core.

Because of the somewhat faster response of the stainless steel-clad reactor, an additional procedural safeguard is proposed to minimize the possibility of occasioning a positive reactor period too short to be safely reversed by the reactor control system. It is proposed that the maximum potential excess reactivity in any loading be limited to less than prompt critical, i.e., to less than or equal to 0.7%. This limitation puts the maximum demand on the control system well below its limitations of performance since a prompt critical period (calculated to be 100 msec by conservative calculation as shown in Fig. 11) is a factor of more than ten slower than the shortest period ($\gtrsim$ 6 msec) within the capacity of the control system to reverse with safety as predicted by the analog calculation.

It is recognized that the determination of the maximum potential excess reactivity may not in every experimental situation be easy to achieve. However, it is proposed that in the first phase of critical experimentation and testing of the BSR-II prior to the SPERT tests, no void tanks, or external reflectors or poisons will be used in the vicinity of the core. With that restriction the only other plausible mechanism for accidentally increasing the reactivity would be the dropping of fuel onto the core, which, as was discussed above, will not result in a harmful excursion, if limited to one fuel element at a time.

As a check on the validity of the calculated behavior of the BSR-II, it is planned to carry out a series of tests on the first BSR-II core at the SPERT facility. It is intended to observe the behavior of the reactor with its control system under step or fast-ramp reactivity insertion in order to measure the limitations of the control system. It is anticipated that owing to the conservative assumptions made in the calculations reported herein, it will become apparent that the actual performance of the system is superior to that claimed here. If this expectation should, in fact, be borne out, a re-evaluation of the loading and operating limits will be undertaken to take fuller advantage of the capabilities of this reactor.

Appendix 1

DECELERATOR DESIGN

The decelerator was designed upon the basis of an analog computer calculation designed to predict the performance of a given decelerator configuration. The equation used to predict the performance of the decelerator is

$$\ddot{S} = K_1 - \dot{S}^2 K_2 \left[\frac{1}{(A_{co} + A_\nu)^2 \; C_\nu^2 C_\delta^2} \right] ,$$

where

$\ddot{S}$ = positive downward acceleration at time t, ft/sec^2,

$K_1 = (W - F_{H_2O} - q)/M$, ft/sec^2,

W = weight of parts in air, lb,

F_{H_2O} = buoyant force of water, lb,

q = dynamic water drag $= \frac{1}{2}\rho \dot{S}^2 A C_D n$, lb,

ρ = density of water, lb/ft^3,

$\dot{S}$ = velocity, ft/sec,

$A = 0.0184$ ft^2,

C_D = drag coefficient,

n = a constant depending on geometry,

M = mass of moving parts, slugs,

$K_2 = A^3\rho/2W$,

A_{co} = area of constant annular orifice formed by clearance between the lift tube and decelerator bushing,

A_ν = area of varying annular orifice formed by clearance between the piston and the wall of the decelerator,

$$= \frac{\pi}{4}\left[\left[D_1 - \frac{S}{S_0}(D_1 - 2.376)\right]^2 - 4.632\right] \Big/ 144 \text{ ft}^2.$$

The terms C_ν and C_δ are the coefficients of velocity of efflux and of discharge for the orifices. The varying annular orifice and the quantities D_1, S, and S_0 are defined as shown in Fig. 13. To design the decelerator, various combinations of D_1 and S_0 were tried in the equations for several assumed values of C_ν and C_δ. The equations were solved on an analog computer and the results were compared for minimum final velocity and most nearly uniform decelerating force. The decelerator finally used in the tests had the dimensions shown in Fig. 13. Although a straightline taper of D_S does not yield the theoretically optimum shape of decelerator wall, it is by far the easiest to fabricate and was used for this reason. The test results showed that the straightline taper approximated the best theoretical curve quite well, since the plate assembly decelerated to a velocity of about 1 in./sec in each case before hitting the stop.

UNCLASSIFIED
2-01-058-0-322

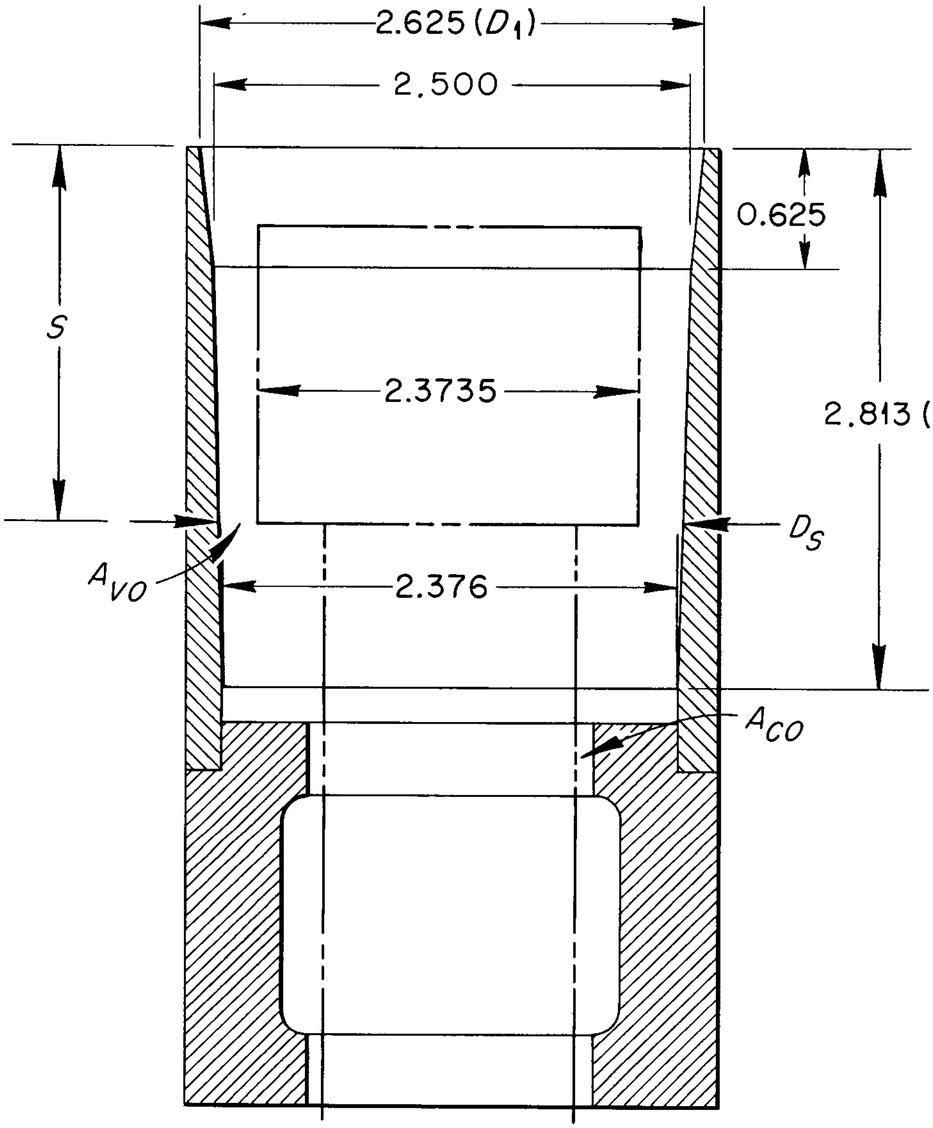

ALL DIMENSIONS ARE IN INCHES

Fig. 13. Cross Section View of the Dashpot Decelerator Designed for BSR-II.

Appendix 2

DESCRIPTION OF CRITICAL MASS CALCULATIONS

The UNIVAC "Eyewash" code is a thirty-group, nine-region, spherical one-dimension reactor code which includes the Goertzel-Selengut model for slowing down in hydrogeneous moderating media. The multigroup equation solved by the code in each region is:

$$-\left[\Sigma_{sH}(u) + \Sigma_a(u)\right] \phi(u,r)du + \frac{1}{3\Sigma_{tr}(u)} \Delta\phi(u,r)du + \xi\Sigma_t(u)\phi(u,r)$$

$$- \xi\Sigma_t(u + du)\phi(u + du, r) + du\, e^{-u} \int_0^u \Sigma_{sH}(u')\phi(u',r)e^{u'}\, du'$$

$$+ \nu_c f(u)du \left[\int_0^{u^{th}} \Sigma_f(u')\phi(u',r)du' + \Sigma_f^{th}\phi^{th}(r)\right] = 0$$

and the corresponding equation for the thermal group is:

$$- \Sigma_a^{th}\phi^{th}(r) + \frac{1}{3\Sigma_{tr}^{th}} \Delta\phi^{th}du + \xi\Sigma_t^{th}\phi(u^{th},r)$$

$$+ e^{-u^{th}} \int_0^{u^{th}} \phi(u',r)\Sigma_{sH}(u')\, e^{u'}\, du' = 0$$

where the following definitions of the symbols apply:

r = radius, cm,

u = lethargy,

Δ = the Laplacian operator,

u^{th} = lethargy boundary of thermal group,

Σ_{sH} = macroscopic hydrogen scattering cross section, cm^{-1},

Σ_a = macroscopic total absorption cross section, cm^{-1},

Σ_t = macroscopic total cross section (excluding hydrogen), cm^{-1},

Σ_f = macroscopic fission cross section, cm^{-1},

Σ_{tr} = macroscopic transport cross section, cm^{-1},

Σ^{th} = macroscopic thermal group cross section, cm^{-1},

ξ = mean lethargy gain per collision,

$f(u)$ = fission spectrum,

$\phi(u)$ = flux per unit lethargy interval, neutrons cm^{-2} sec^{-1},

ϕ^{th} = thermal flux in neutrons, cm^{-2} sec^{-1},

ν_c = number of neutrons per fission needed to make the assembly critical.

It will be observed that the treatment is a straightforward group-diffusion treatment except for the hydrogen effect. The hydrogen is treated as a scattering material which will throw the scattered neutrons into a lower group with a probability of lethargy gain Δu proportional to $e^{\Delta u}$. This is the Goertzel-Selengut method. All other energy degradation is assumed to occur in incremental steps that take a neutron into the next lower lethargy group after a number of collisions $\Delta u/\xi$. This method, then, does not take any account of the inelastic scattering processes that could take a neutron from a high energy directly to a much lower one. Since this effect is only of the magnitude of a few percent, however, it would not affect the relative results in the parametric study of the effects of fuel content and numbers of plates per element; it has been omitted from consideration.

The code requires as input the specification of the dimensions of each spherical shell in terms of the number of regions of thickness Δr, where Δr is the one-dimensional mesh used in the calculation. These shell thicknesses are arbitrarily specified in the input within the limitations that the total number of mesh points be no more than 60, and that the ratio of cross sections in adjacent regions is neither greater than 10, nor less than 0.1. The latter restriction is in any case necessary since its violation would render a diffusion theory calculation meaningless.

The other part of the input consists of specifying the nuclear species, and the concentrations of each species present in each of the up to nine regions. There may be as many as seven such nuclear species in each region.

The code contains tabulated cross sections for each material in its tape memory, and it constructs the necessary cross sections from these data and the concentrations.

It is to be observed that this procedure results in treating the material in each region as a monoatomic gas, neglecting all binding effects unless, as was not done here, adjusted cross sections are introduced to include binding effects. Neglecting binding effects introduces some error at low energy, but past experience with this code in calculating BSR-I cores has shown that, due to the fact that most transport in aqueous systems is fast transport, resulting error is small.

A further input datum is provided for in order to allow for the effect of self-shielding in fuel plates. The code considers the materials in each region to be homogeneously distributed, which would mean an error in the case where fuel is arranged in slabs that cause partial self-shielding. Therefore, a number

$$L_R = \frac{0.321 \text{ x Fuel Plate Thickness}}{\text{Fuel Plate Volume Fraction}}$$

can be specified for each region R, from which the code determines a self-shielding factor, f_i, for each energy group, i, given by:

$$f_i = 1 - L_R \, N(25) \, \sigma_a^i(25)$$

where

$N(25)$ = concentration of U^{235} atoms per cm^3 of the region,

$\sigma_a^i(25)$ = microscopic absorption cross section of U^{235} averaged over the i-th energy group.

This factor corrects for the self-shielding inside the fuel plate, but does not take the small flux deformation in the space between fuel plates into account.

The completely reflected parallelepipedal shape of the BSR-II has to be equated with a series of concentric spherical regions capable of being calculated with the code. The transformation was made by means of the Prohammer method[6] as extended by E. G. Silver.[7] This method consists of finding the buckling of the parallelepiped with reflector savings added, and then subtracting the same reflector savings from the sphere radius which yields the same buckling. The reflector savings is a thermal reflector savings given by

$$\partial = (D_c/D_r)L_r$$

where

D_c, D_r = thermal diffusion coefficients in the core and reflector, respectively,

L_r = diffusion length in the reflector.

This formula is the "large core" limit of a more general formula given in section 8.25 of "The Elements of Nuclear Reactor Theory" by Glasstone and Edlund.[8]

The entire core region of the reactor was homogenized, including the eight channels for the control plates. These channels are narrow enough so that the flux rise in their vicinity will not be very large, and thus the simplification is valid.

The BSR-II will have a rather large amount of stainless steel close to the core in the form of the lower end boxes and the grid plate. There will also be poisons near the top of the core in the form of the upper extensions of the side plates, the handles, and in the lower ends of the poison plates which are inserted into the upper edge of the core. These materials have been included in the calculation by finding their effective homogeneous cross section (taking self-shielding in the thick members into account) and then spreading this amount of material into a uniform circular shell around the core region. Three such shells of thicknesses Δr, $2\Delta r$, and Δr were included.

The core region of the reactor was assumed to consist of U^{235}, stainless steel, oxygen (from the water and also the UO_2), and hydrogen. The U^{235} cross sections are already adjusted for the 93% enrichment to be used in the BSR-II so that no explicit allowance for the presence of the U^{238} was necessary.

The shell regions contain water and stainless steel and, in one case, water, stainless steel, and boron. The reflector region is pure water.

The concentrations of steel and UO_2 in the core were calculated as follows: For each case considered, the number of fuel plates per element, the thickness of the fuel region, and the fuel region area per fuel plate gives the total fuel volume in the core. The density of the fuel material was assumed to be 0.92 of theoretical density, and the volume fractions of the two constituents of the "meat" are computed to give the desired amount of U^{235} in the core. Since the result of the calculation is a value of ν_c, for a given amount of fuel put in, a range of calculations is necessary for each core design with different amounts of fuel, steel, and oxygen, in order to determine by graphical analysis the amount of fuel needed for criticality.

In order to find the best choice of parameters, a variety of choices of fuel region thicknesses and number of fuel plates per element are considered. The results are presented in the body of this report.

Table 4 lists the input parameters and some cross sections for the design point calculation.

Figure 14 shows the distribution in energy of the neutrons initiating the fissions as calculated; it also shows the corresponding information for the BSR-I and for a 1-ft cube core of steel which was considered for BSR-II.

Table 4. Data for Calculation 557159

Amount of Enriched Uranium (93% U^{235})	5.9 kg
Equivalent Number of Plates per Fuel Element	20
Equivalent Fuel Plate Thickness	0.030 in.
Cladding Thickness	0.008 in.
Number of Regions in Calculation	5
R Step (Radial Mesh Spacing) (Δr)	0.871 cm
Core Radius in Δr Units	26
Shell 1 Thickness in Δr Units	1
Shell 2 Thickness in Δr Units	2
Shell 3 Thickness in Δr Units	1
Reflector Thickness in Δr Units	30
Uranium Concentration in Core	2.68×10^{20} atoms/cc
Stainless Steel Volume Fraction in Core	0.210
Stainless Steel Volume Fraction in Shell 1	0.081
Stainless Steel Volume Fraction in Shell 2	0.139
Equivalent Natural Boron Concentration in Shell 2	1.41×10^{19} atoms/cc
Stainless Steel Volume Fraction in Shell 3	0.121
Equivalent Temperature of Thermal Group	66°F
Thermal Absorption Cross Section in Core	0.242 cm^{-1}
Calculated ν_c	2.478
Thermal Fission Cross Section in Core	0.141 cm^{-1}
Thermal Transport Cross Section in Core	1.29 cm^{-1}

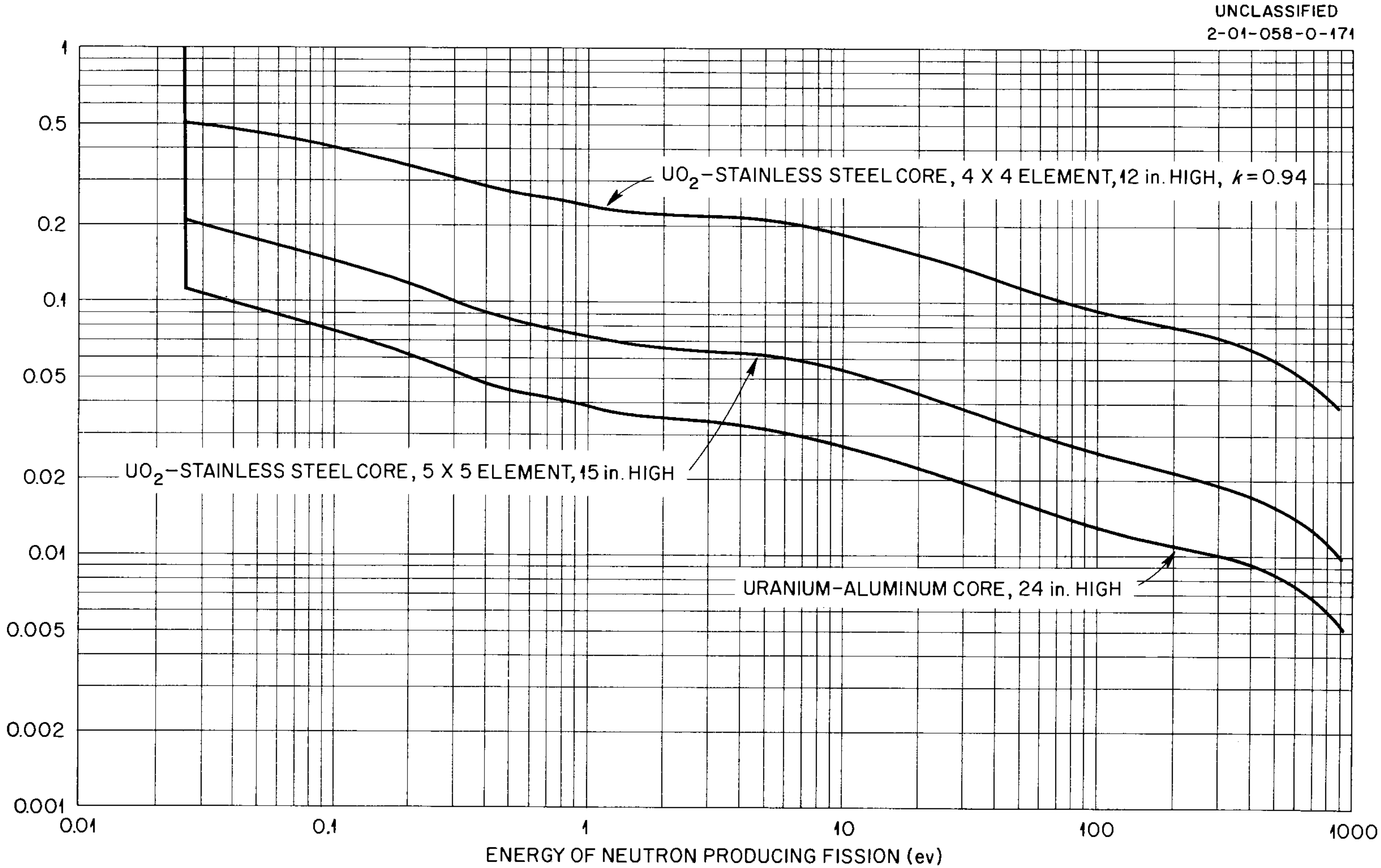

Fig. 14. Fraction of all Fissions Initiated by Neutrons Above Energy, E, as a Function of Energy, E; as Calculated by the "Eyewash" Code. The three curves are the results for the BSR-I (bottom curve), the BSR-II (middle curve) and a steel reactor designed for a one cubic foot core which was abandoned because of its large epithermal fission fraction (upper curve).

Appendix 3

DETAILS OF HEAT TRANSFER CALCULATIONS

A calculation was carried out to determine the maximum power level at which the core could be operated without the occurrence of local boiling at the hottest point in the fuel elements. This calculation was made by a method of successive approximations of the average water density in the central fuel element as follows:

(1) $$dQ_z = q_z A dz \text{ (Btu/hr)}$$

(2) $$Q_z = xC_p(T_z - T_0) \text{ (Btu/hr)}$$

(3) $$x = A_w \nu_z \rho_z \text{(lb/hr)}$$

(4) $$\nu_z = \left[2\left(\frac{\rho_0 - \bar{\rho}_z}{\bar{\rho}_z}\right) gz\right]^{1/2} 3600 \text{ (in./hr)}$$

where

Q_z = total heat transferred to water in length z of fuel elements, Btu/hr,

q_z = heat generation rate at any point z in central fuel element, $\text{Btu}\cdot\text{hr}^{-1}\cdot\text{in.}^{-3}$,

A = gross cross section of fuel element, in.^{2},

z = length of fuel element, in.,

x = mass water flow, lb/hr,

C_p = heat capacity of water, $Btu \cdot lb^{-1} \cdot (^{\circ}F)^{-1}$,

T_z = mean water temperature at point z, $^{\circ}F$,

T_0 = water temperature in pool, $^{\circ}F$,

A_w = cross section available for water flow, in.^{2},

ν_z = average velocity of water flow over area A at point z, in./hr,

ρ_z = water density at point z, corresponding to temperature T_z, lb/in.^{3},

$\bar{\rho}_z$ = average water density in length z, lb/in.^{3},

g = acceleration of gravity, in./sec^2.

The calculated flux shape in the core was then approximated with a cosine distribution of which only a central part was used. The portion used was chosen to have the same peak-to-average flux ratio as that of the calculated flux shape, as shown in Fig. 8. This ratio was 1.89:

$$q_z = \frac{1.89P}{3300} \sin\left(\frac{\pi z}{15}\right) \quad (Btu \cdot hr^{-1} \cdot in.^{-3}) \tag{5}$$

where P is the reactor thermal power level, in Btu/hr.

The method used was to find the value Q_z by use of Eqs. 1 and 5; x was then plotted as a function of $(T_z - T_0)$. A value for $(T_z - T_0)$ was then assumed, and a value of $\bar{\rho}_z$ was obtained from a curve of ρ vs T. Using this value of $\bar{\rho}_z$, a value of ν_z was found from Eq. 4, after which a value of x was found from Eq. 3. This x, substituted back into Eq. 2, should yield the original $(T_z - T_0)$. If it did not, a new value of $(T_z - T_0)$ was assumed, and resultant temperature differences were checked.

The temperature of the fuel plate surface was then found from

(6) $$T_w = \frac{Q_z}{ha} + \bar{T}_z$$

where

T_w = fuel plate wall temperature at point z, ^oF,

h = average heat transfer coefficient over length z, $Btu \cdot hr^{-1} \cdot (^oF)^{-1} \cdot ft^{-2}$,

a = surface area available for heat transfer in length z, ft^2,

$\bar{T}_z$ = average fluid temperature over length z, ^oF.

With 20 fuel plates per elements, the plate surface temperature, T_w, in the central fuel element was found to reach 239^oF, the boiling point for water under a head of 20 ft at a reactor power of about 1000 kw, Fig. 15. The effective transfer coefficient h was 140 $Btu \cdot hr^{-1} \cdot (^oF)^{-1} \cdot ft^{-2}$. At this same power level, the average water temperature rise in passing through the fuel element was 42^oF (Fig. 16). Thus the stainless steel-clad reactor would be limited in power level to below 1 Mw. Based on past experience with the aluminum-clad core, it is not anticipated that such a power level limitation would present any difficulties for the performance of shielding experiments.

An identical calculation for loading No. 33 of the aluminum-clad BSR-I was compared with measured temperatures of the water. Good agreement was obtained, well within experimental accuracy. The measured wall temperatures however, indicate that a heat transfer coefficient of 140 $Btu \cdot hr^{-1} \cdot (^oF)^{-1} \cdot ft^{-2}$ is conservative.

UNCLASSIFIED
2-01-058-0-314

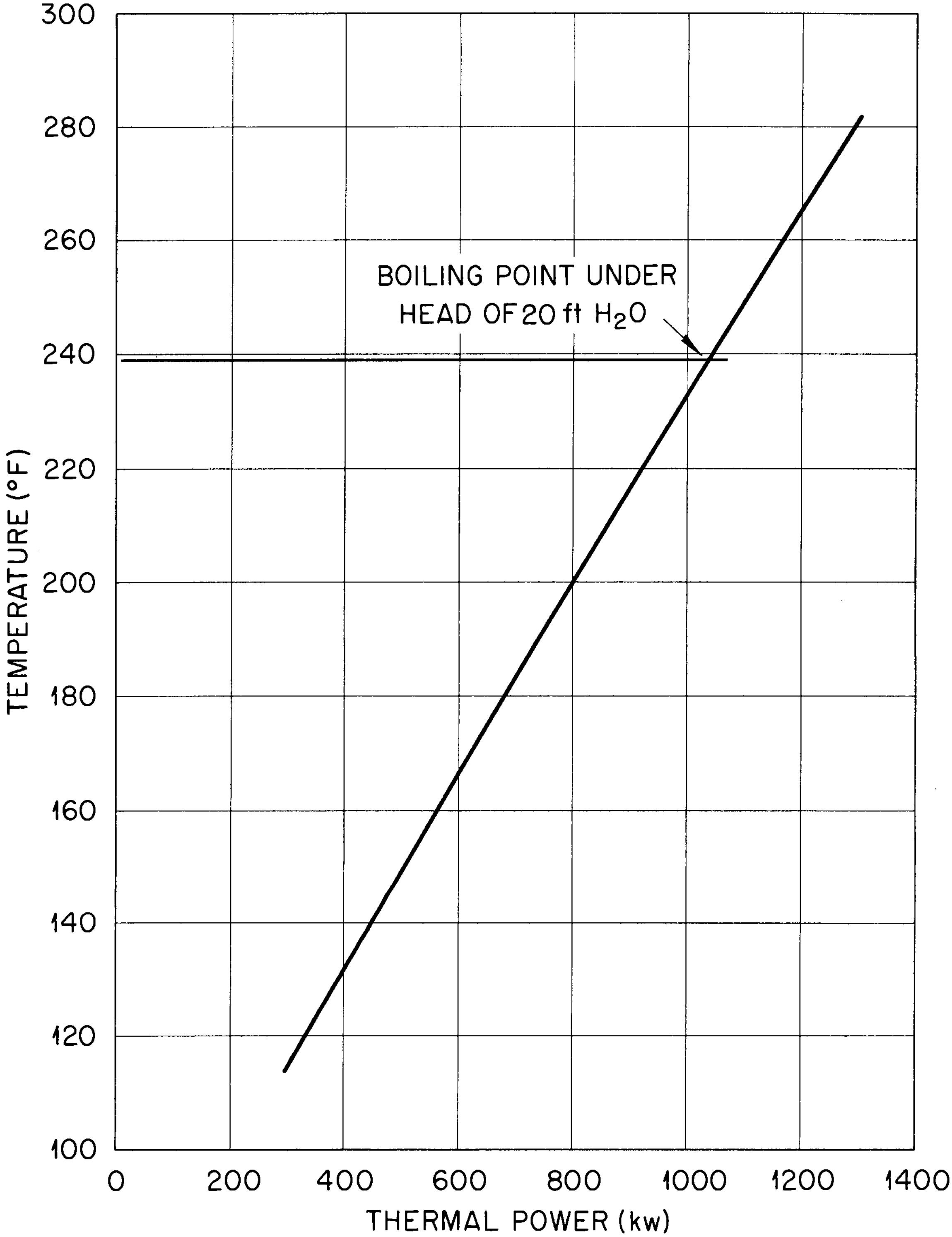

Fig. 15. Calculated Fuel Plate Surface Temperature at Hottest Point in the BSR-II as a Function of Reactor Power.

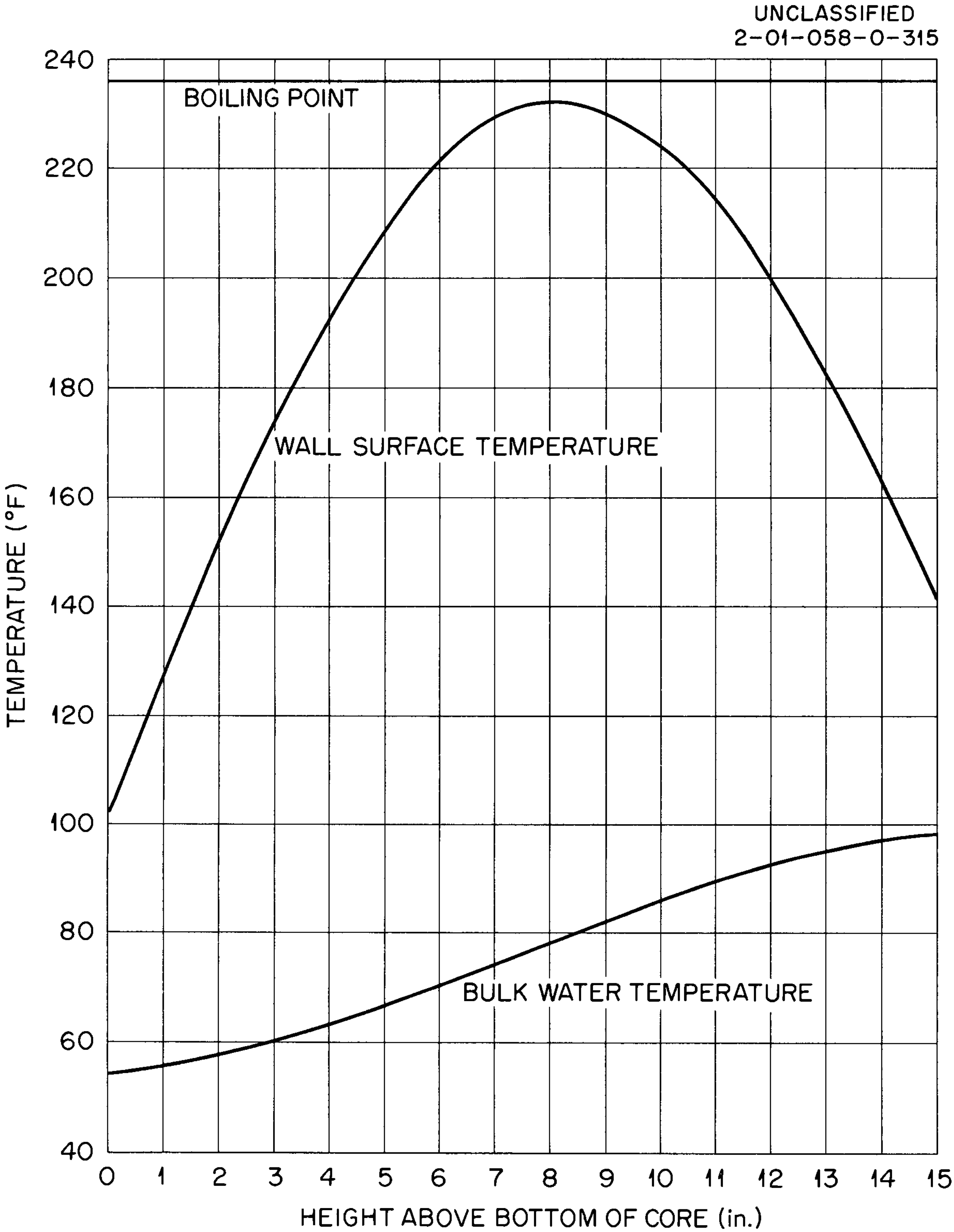

Fig. 16. Calculated Fuel Plate Surface Temperature, and Bulk Water Temperature as a Function of Height Above the Bottom of the Core in Inches, for the Central Water Channel in the BSR-II at a Power of 1.0 Megawatt.

Appendix 4

CONTROL PLATE TESTS IN BSR-I

In order to determine the effect of the flat control plates in the BSR-II, a series of tests was carried out in the BSR-I with plates of aluminum containing a dispersion of B_4C with natural boron.[9] It was desired to determine the effect, at the center of the BSR-I, of a plate equivalent to the plates designed for the BSR-II. To calculate this effect it was assumed that a plate containing a given areal density of B^{10} will have the same effect in a core 15 in. high as in a core 24 in. high if it extends the full height of the core in both cases.

Since the BSR-II plates are to contain 4.5 g of boron of which 90% is B^{10}, whereas the plates tested in BSR-I contained natural boron (18.8% of B^{10}), the equivalent amount of boron in the BSR-I test plates is:

$$(24/15)\ (90/18.8)\ 4.5 = 34.5 \text{ g}$$

An experiment was done using Loading 64 of the BSR-I. This configuration is shown in Fig. 17. It contains 28 fuel elements of which four are control rod elements. A special fuel element containing a number of removable plates was placed either in position 14 or in position 24 (the other position containing a regular fuel element). One plate in the special fuel element was removed and replaced with the test plates containing boron. Figure 17 shows the $\Delta k/k$ per gram of boron for various boron content plates in the two slots indicated. Only in position 14 was it possible to extend the experiment

UNCLASSIFIED
2-01-058-0-316

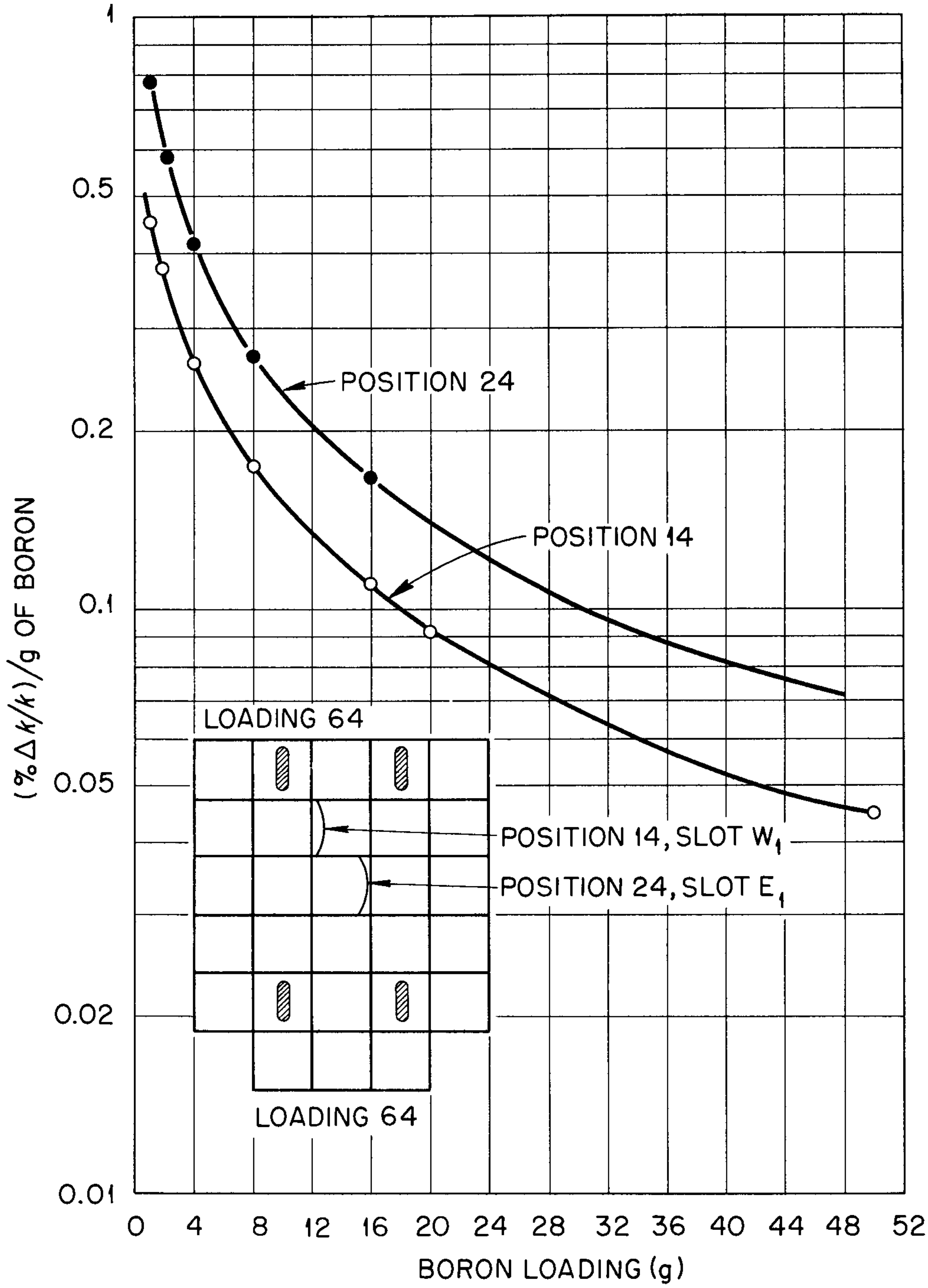

Fig. 17. Per Cent Change of Reactivity Per Gram of Natural Boron as a Function of Amount of Boron Measured in a Single Plate in the Eastmost Slot of Position 24, and the Westmost Slot of Position 14 of Loading 64 of BSR-I. The shape of loading 64, as well as the locations of the experimental slots therein are shown in the diagram. The gray areas in the diagram represent control rods. The measured points are shown by circles. The lines represent interpolation between the measured values.

to the maximum of 50 g of boron. Therefore, the data for the center position (position 24) were extended by comparison with the position 14 data, as shown in the figure. The result of the extrapolation is 0.092% $\Delta k/k$ per gram of boron with 34.5 g in position 24 in the slot designated as E_1. This means a total worth of 3.1% $\Delta k/k$ for a plate at this point. To determine the effect at the actual center of the loading a test was made in which each of the available slots in position 24 was tested in turn with an 8-g boron plate and a 16-g boron plate. The exact center position is not available for measurement, but an interpolation of data taken from either side of center was made, as shown in Fig. 18. The interpolation yields a factor of 1.042 as the ratio of center position to position E_1 effectiveness. This gives a result of 3.30% as the worth of a BSR-II equivalent boron plate at the center of the BSR-I as compared with a water space in that position.

The transmission of a B^{10} plate was calculated on the assumption that the boron is uniformly dispersed in the plate. The result is given in Fig. 19. The two curves represent the transmission for (1) perpendicular incidence of the neutrons and (2) transmission from an isotropic volume source on one side of the plate. It is observed that the transmission of the design plate is of the order of 1%. It is expected, though, that due to the particulate nature of the boron in the control plate the transmission will be as much as 5% rather than the 1% calculated, assuming homogeneous distribution.

An experiment was also carried out to determine the effect of pairing two control plates with various separation distances between them. The

UNCLASSIFIED
2-01-058-0-318

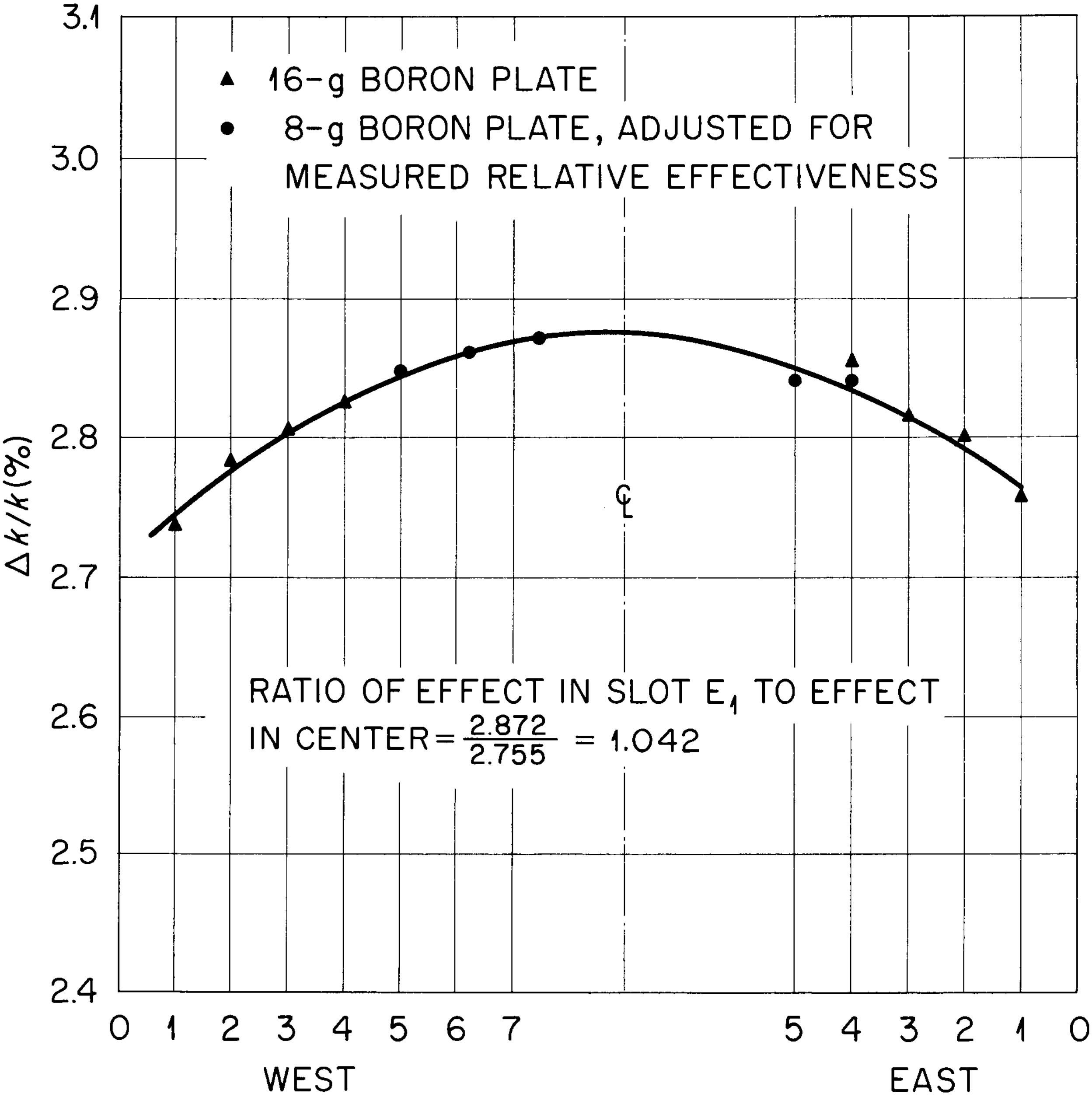

Fig. 18. Measured Effectiveness of a Single Plate Containing Boron as a Function of Its Location in Position 24 of Loading 64 (Fig. 17). The measured points were obtained in each of the plate positions of 12 movable fuel plates in a special fuel element. The reactivity is compared with that for fuel plates in all slots. The measurements were made with fuel in all slots but the one containing the boron. The abscissa gives the number of the slot used, counting from east and west side inward.

UNCLASSIFIED
2-01-058-0-317

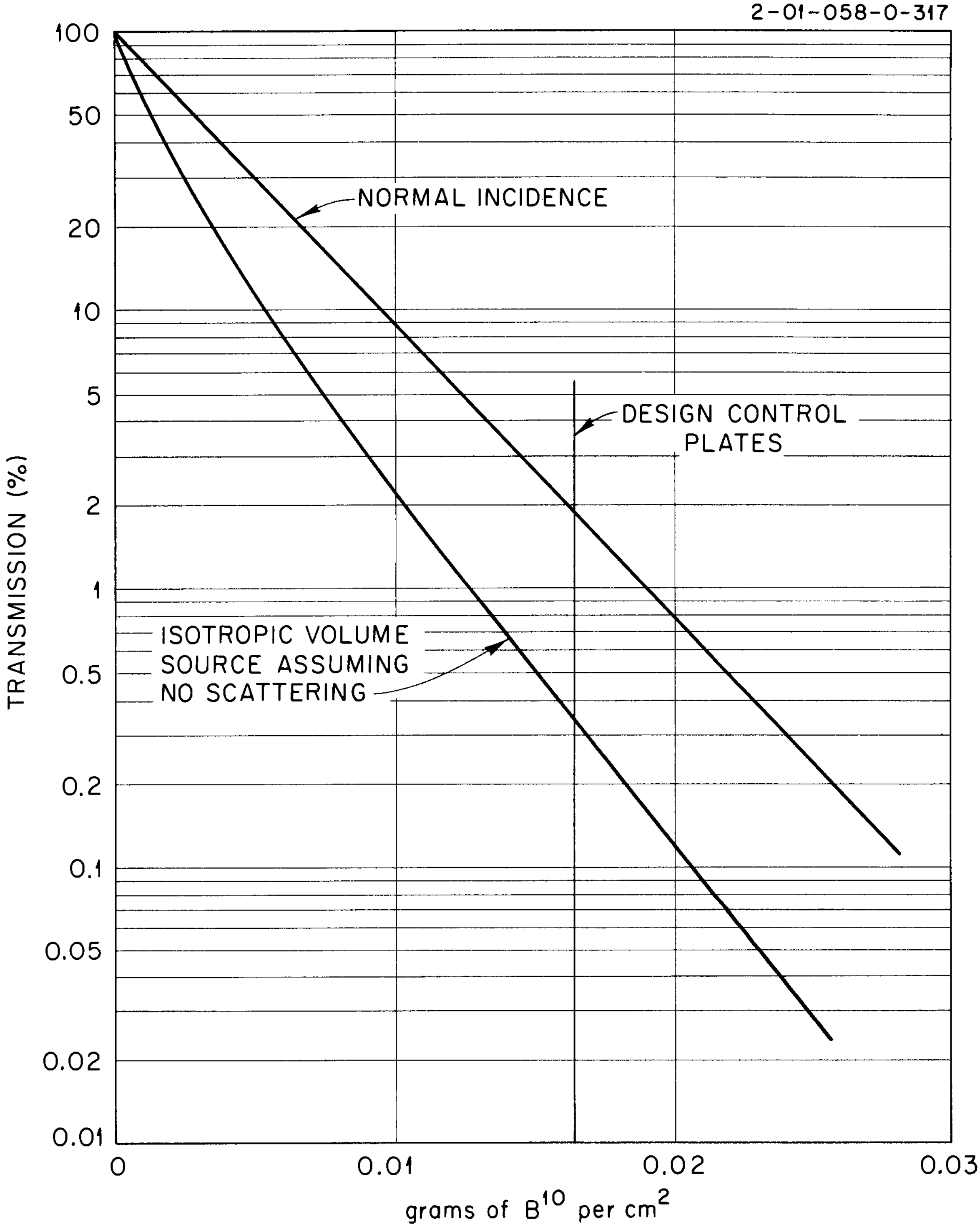

Fig. 19. Calculated Thermal Neutron Transmission of a Thin Plate of Homogeneously Distributed B^{10} Assuming Either Normal Incidence on the Plate, or Isotropic Volume Source Distribution, as a Function of Areal Density of B^{10}.

experiment was performed in position 24 of loading 64 of the BSR-I, using two 2-g boron plates at various separation distances. The results are shown in Fig. 20. In this case the reported %$\Delta k/k$ is for a comparison with fuel in the slots, not water. Therefore, it is not possible to compare this result directly with the result of the single plate experiment where the results are given as compared to water in the test slot. However, the following additional data permits a comparison: In the two most widely separated slots, E_1 and W_1 (6.7 cm apart), measurements were taken with one and two plates containing boron, with water in the unused slots, as follows:

Boron plates in both slots: excess k = 0.39%

Water in both slots: excess k = 2.75%

Boron in one slot and water in the other: excess k = 1.56%

The reactivity held by one 2-g boron plate is then 2.75 - 1.56% = 1.19% and the effect of two boron plates is 2.75 - 0.39% = 2.36%. The effect of two plates is almost exactly twice the effect of a single plate. Looking at the curve in Fig. 20 it is seen that this separation effect saturates for distances greater than 4 cm. The separation of the two control plates of a single control element in the BSR-II is 7.08 cm and one may thus conclude that interaction between two such plates is not a strong effect. It is true that the test was made with plates having a reactivity effect of about 1.2% each, and the result is applied to plates having a reactivity effect of 3.3%; however, the separation distance is 1.75 times as great as the minimum separation distance for no observable interaction as measured, and the BSR-II,

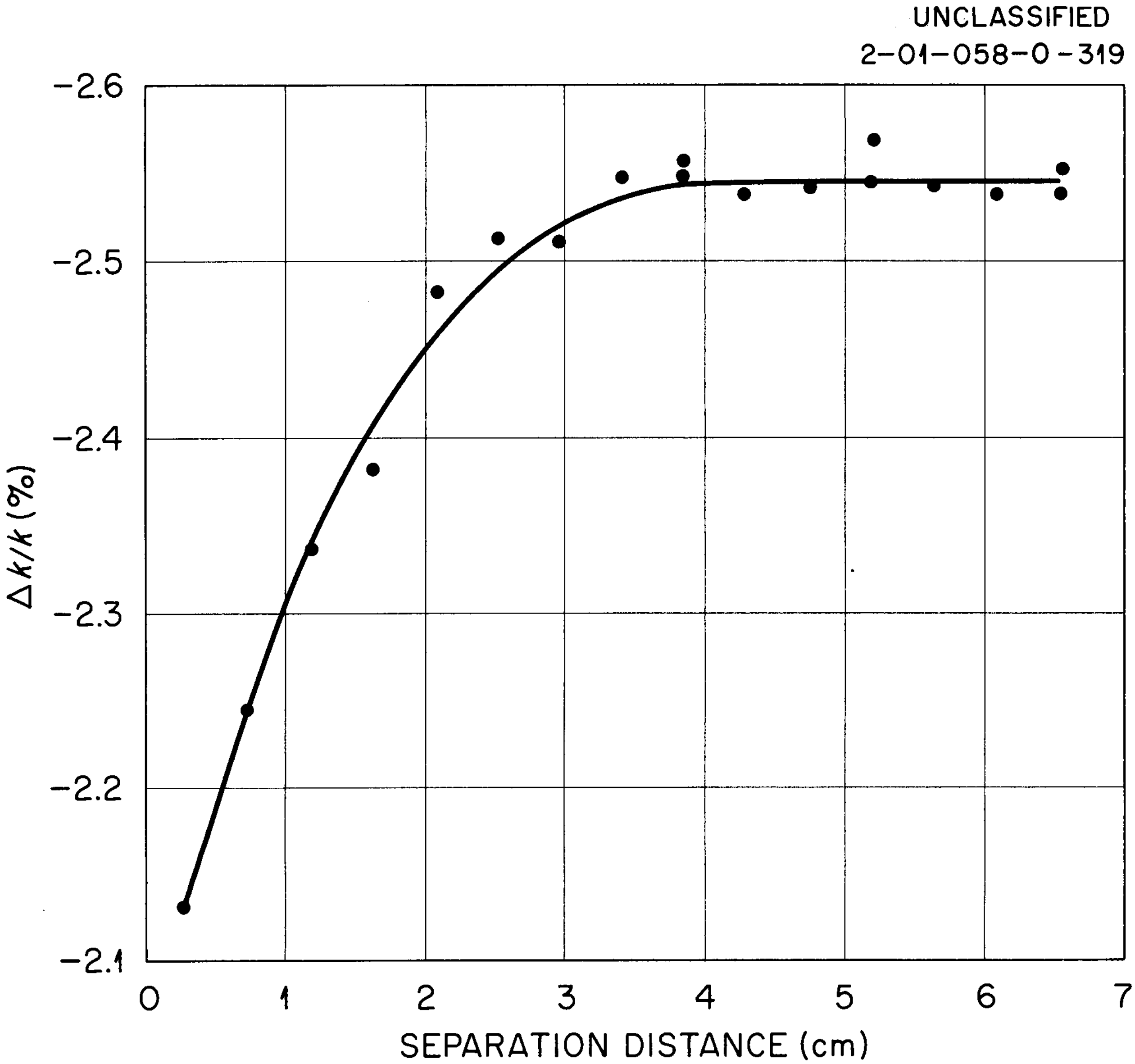

Fig. 20. Per Cent Change in Reactivity Caused by Insertion of Two Plates, Each Containing Two Grams of Natural Boron, into Position 24, Loading 64 of BSR-I Compared with the Reactivity with Fuel in all Slots, as a Function of Separation Distance Between the Plates.

having a higher absorption cross section than BSR-I, has a shorter neutron diffusion length, so that the interaction effect should be less, for the same geometric separation, than in the BSR-I.

Appendix 5

CONTROL PLATE DROP TESTS

In order to evaluate the effectiveness of the designed control rod drive mechanism a mockup of the entire assembly was tested to obtain experimentally the information needed to evaluate the safety condition of the reactor in case of a "scram" situation.

A vertical steel tank with one face of plexiglas was used for the test. This tank could be filled with water, the control plate system mounted in it, and its behavior observed through the plexiglas wall with convenience and precision.

The test was carried out with a control plate of somewhat different design than the final design presented in Section I of this report, but the differences are concerned only with the location of the control plate stiffening strip which was at each edge of the plate tested here and is now designed to be at the center of the plate. The weight and dimensions of the plates of both designs are identical, and the clearances between each plate and its channel are almost the same.

Figure 21 shows the entire assembled rig without the plexiglas plate bolted to the front. The portion below the lower cross member of the tank is the mockup of the two control plate channels. Figure 22 shows a close-up of the lower end of the lift tube with the upper ends of the two control plates attached. The index marker on the channel mockup and left-hand control plate also may be seen. These markers were used to record the

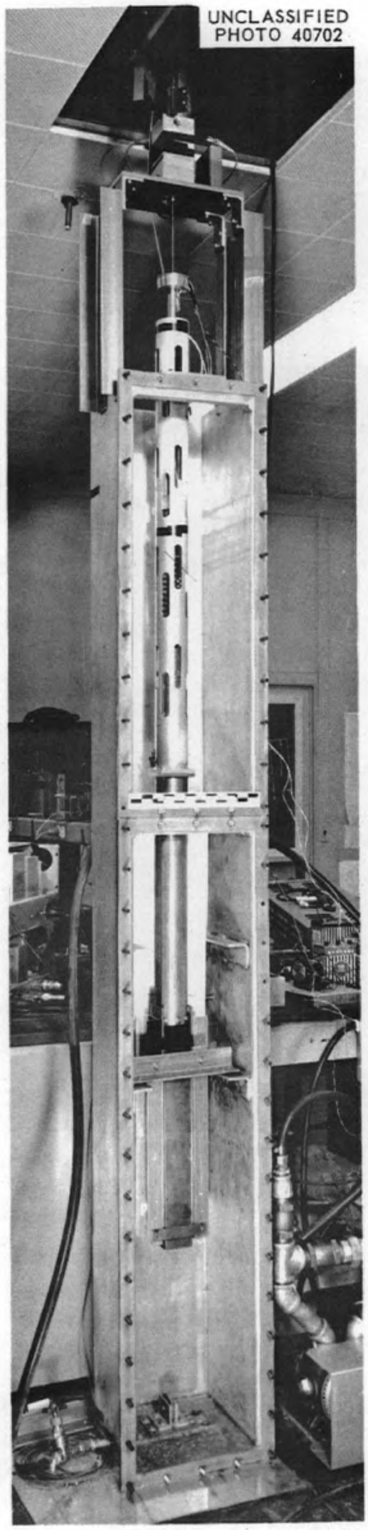

Fig. 21. View of Water Tank in Which the Drop Tests of the BSR-II Control System were Carried Out. The face plates of plexiglas, which permit filling the tank with water during the test is not in place; neither is the Fastax camera used to observe the test results. The control system is in place.

UNCLASSIFIED
PHOTO 40701

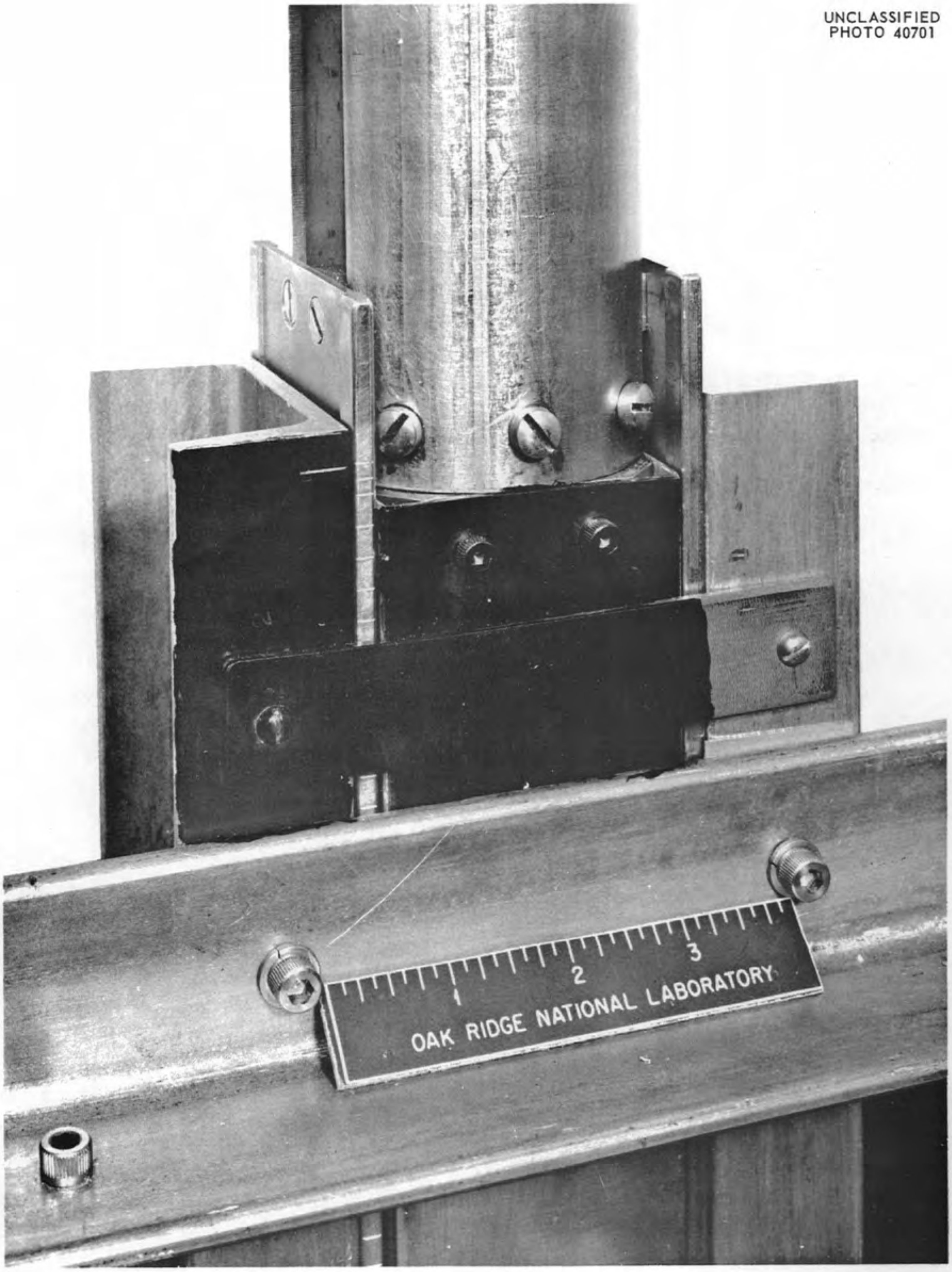

Fig. 22. Closeup View of Upper End of the Two Control Plates with Their Yoke Used in Mechanical Drop Tests of BSR-II Control System. The graduation marks on one plate may be seen. The two U-shaped members mock up the channel wall of the control plate slots.

position of the plate as a function of time as described below. Figure 23 shows a view of the upper region of the lift tube. During the tests a plexiglas plate was bolted to the face of the test tank, which was filled with water at room temperature. All working parts were thus immersed in water.

In order to measure plate position vs times, a Fastax camera running at 2000 frames/sec was used to photograph simultaneously the graduated edge of one of the control plates and the face of a disk rotating at 3600 rpm. In addition, two lamps were placed in the field of view of the camera. One lamp flashed when the magnet current was cut off, and the other flashed when the clutch switch opened, thus indicating that the control-plate assembly had begun to move. The time interval between the flashing of the magnet lamp and the clutch switch lamp represents the time required for the magnet to release plus any overtravel in the clutch switch.

A record of the motion was thus obtained. The film could be read with an accuracy of ± 0.15 turn of the timing disk and, since each full turn of the disk represents 0.0167 sec, the accuracy with which the motion could be determined was ± 0.0022 sec. The position of the control plate could be read on most of the films with an accuracy of $\pm 1/16$ in. or better. The plates were dropped under the following conditions:

1. Initial spring compression to a force of 66 lb, decaying to zero in 3.3 in. (8.2 g) (design case);

2. Initial spring compression to a force of 86 lb, decaying to zero in 4.3 in. (10.2 g);
3. Fall under force of gravity only;
4. Fall under force of gravity only, with one control plate removed from the assembly;
5. Fall under force of gravity only, with both control plates removed from the assembly; that is, only the lift tube, yoke, piston, and magnet armature were dropped.

In addition, the tests were further divided into two parts, with different details for the upper guide tube and the plate lift tube. In the first tests the upper guide tube had no openings in the lower 6 in. of its length, and the lift tube had no openings at its upper end, so that the water inside the lift tube was trapped. Since it was felt that the lack of openings for water passage might affect the motion of the plate assembly, and particularly the performance of the decelerator, the additional holes were cut and the tests repeated. The results showed that this induced only an insignificant change in the control-plate motion.

The main results of this experiment are embodied in Fig. 9 in Section IV of this report. Figure 24 shows the velocities as a function of time after the scram signal for several cases of interest.

A further series of tests with the final design of the control plate will be carried out, as well as a series of drops in order to life-test the system. It is planned to provide for an automatic cycle of

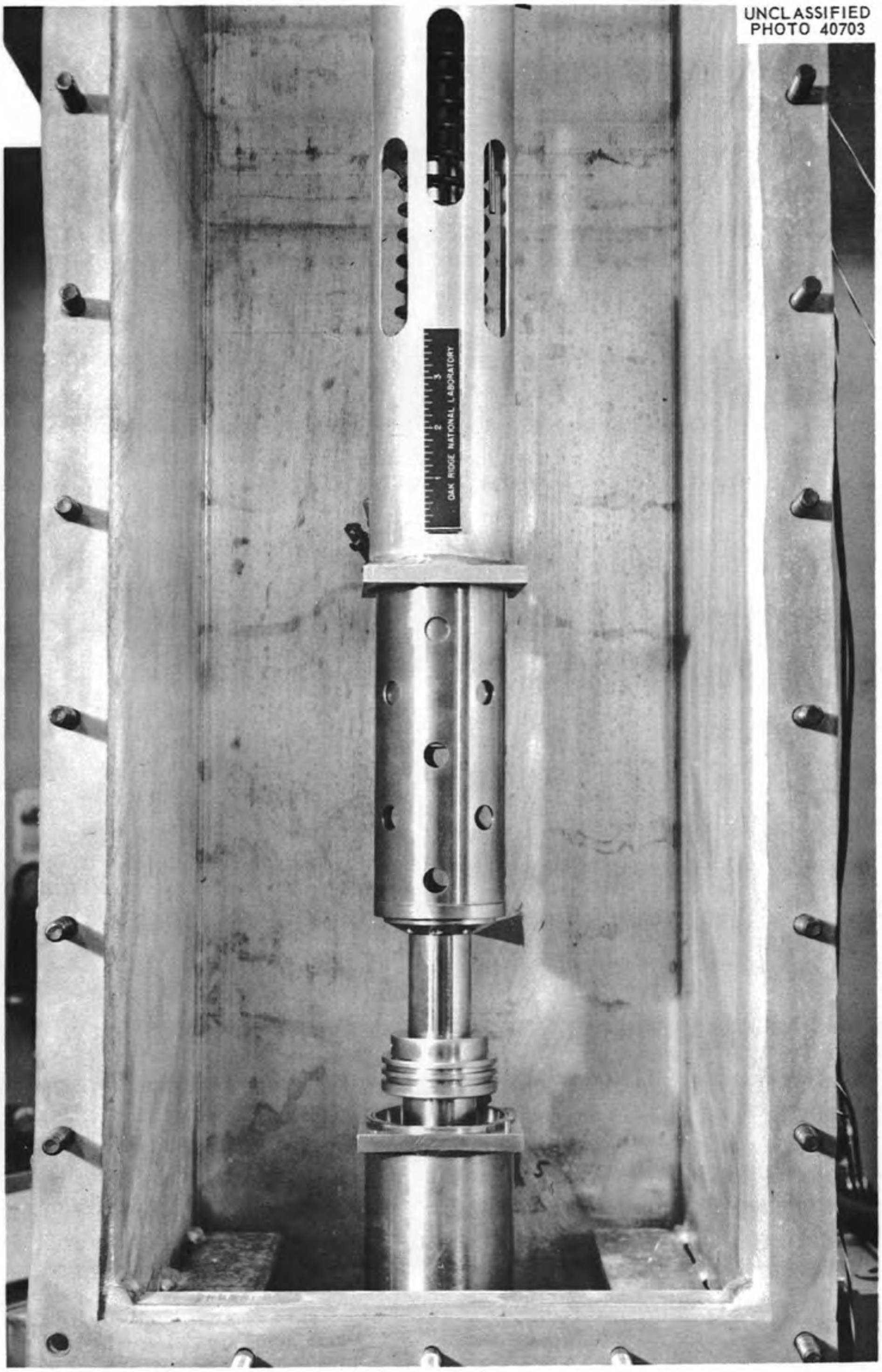

Fig. 23. Photograph of the Partly Disassembled Control Mechanism of BSR-II. The decelerator piston is shown just above the dashpot. Just above it is the upper termination of the lift tube with the armature attached. Resting upon that is the accelerator tube (pierced by circular holes). Inside this tube the magnet may be glimpsed. The outer support tube (pierced by vertical slots) has been drawn upward from its position against the dashpot body. Inside it the accelerator spring is visible.

UNCLASSIFIED
2-01-058-0-324

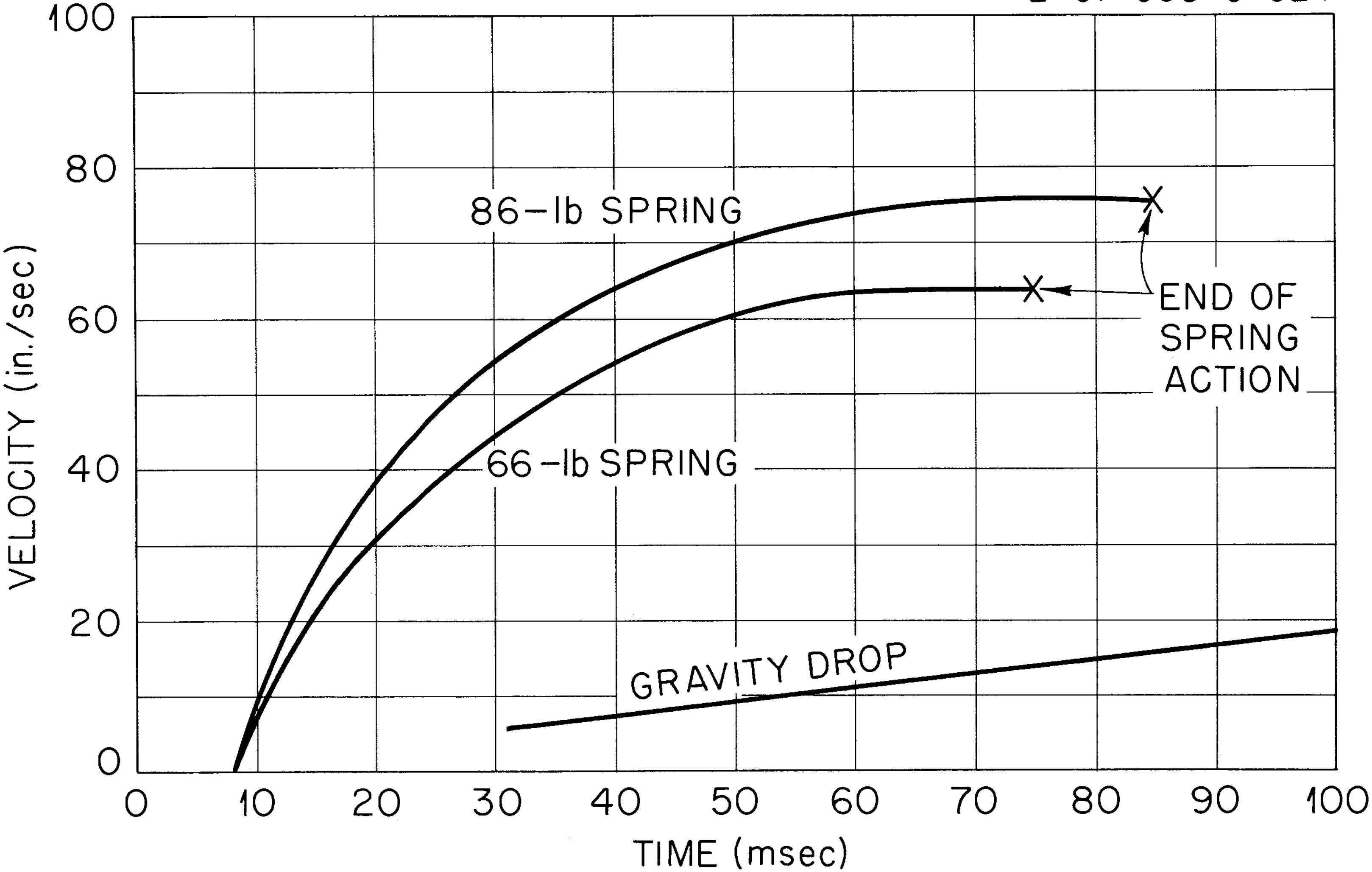

Fig. 24. Control Plate Velocity as Measured in BSR-II Drop Tests as a Function of Time After Scram Signal. The design spring case with 66 lb initial force is shown; as is a gravity drop test, and an 86 lb spring test for comparison.

raising the control system, scramming, lowering the magnet to re-engage the system and raising it anew. A large number of these cycles will be carried out in order to assure the reliability of the design. This test will precede construction of the reactor.

Appendix 6

ANALOG SIMULATION TO DETERMINE THE EFFECTIVENESS OF THE BSR-II CONTROL PLATES IN SUPPRESSING A POWER SURGE*

A determination was made of the shortest reactor period that the proposed BSR-II control plates will counteract before excessive power excursion occurs. The study technique used was based upon the simulation system described in ORNL-2318, in the article "Analogue Simulation of Corrective Action for a Nuclear Excursion."

In this technique, the reactor is initially maintained critical at a low power level. A calibrated positive reactivity step function is inserted, and at an arbitrarily predetermined power level a programmed reactivity decrease is initiated. By a sequence of runs, the exact step function is found which can just be reversed within a power excursion of three decades rise. It is then convenient to repeat and record the excursion with no corrective action in order to measure the stable period induced by the step function.

The variation of reactivity removed with control plate insertion follows the standard sensitivity curve typical of the BSF type reactor. A parameter study was made using total worth in terms of $\Delta k/k$ in the control plates of 4, 6, 8, and 10%, and rod position versus time curves for two initial spring forces of 66 and 86 lb. The latter two curves are shown in Figs. 25 and 26.

*By F. P. Green.

UNCLASSIFIED
2-01-058-0-370

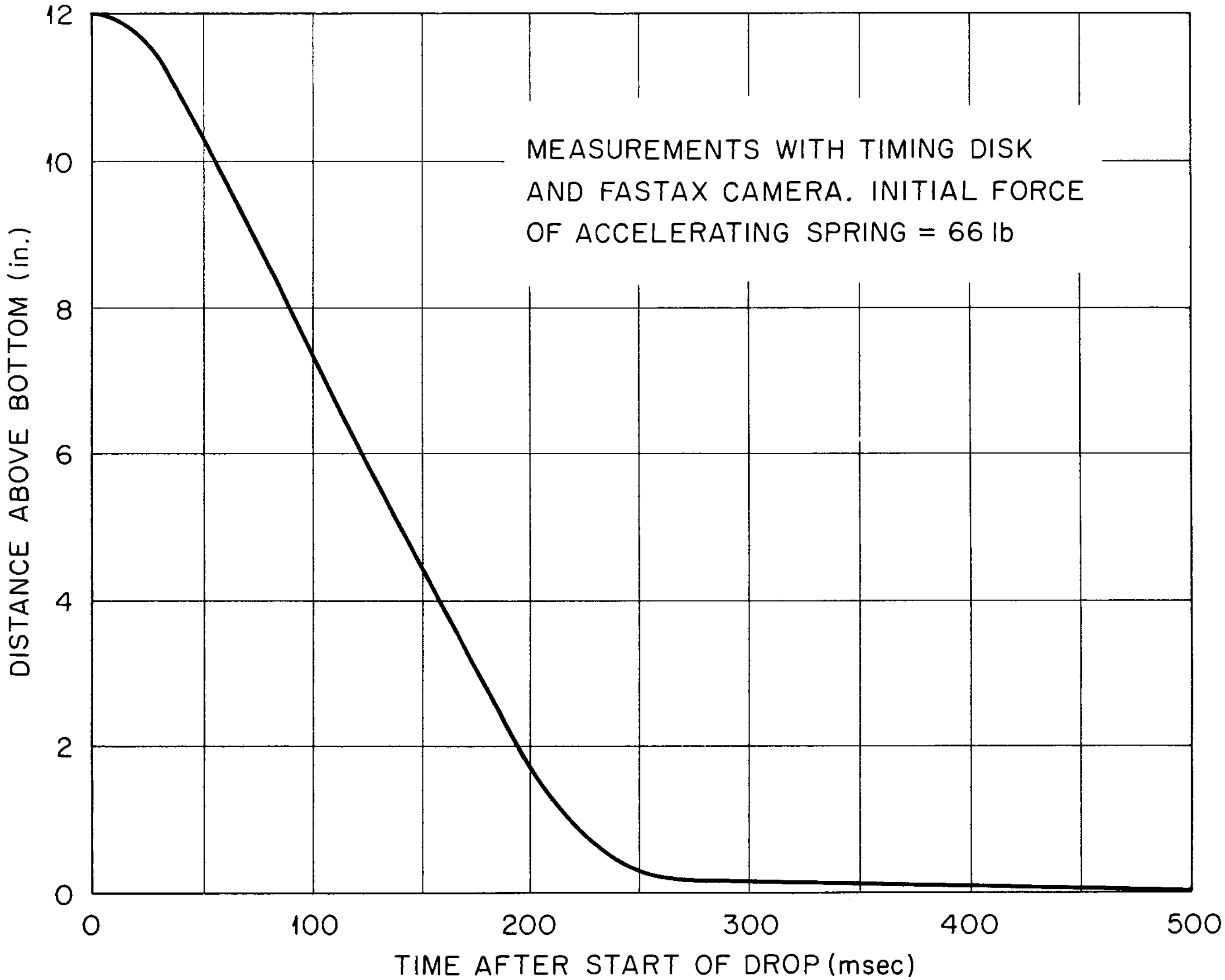

Fig. 25. Position of BSR-II Control Plate Lower Edge as a Function of Time After Start of Drop, as Measured with Timing Disc and Fastax Camera. The accelerating spring had an initial force of 66 lb.

UNCLASSIFIED
2-01-058-0-371

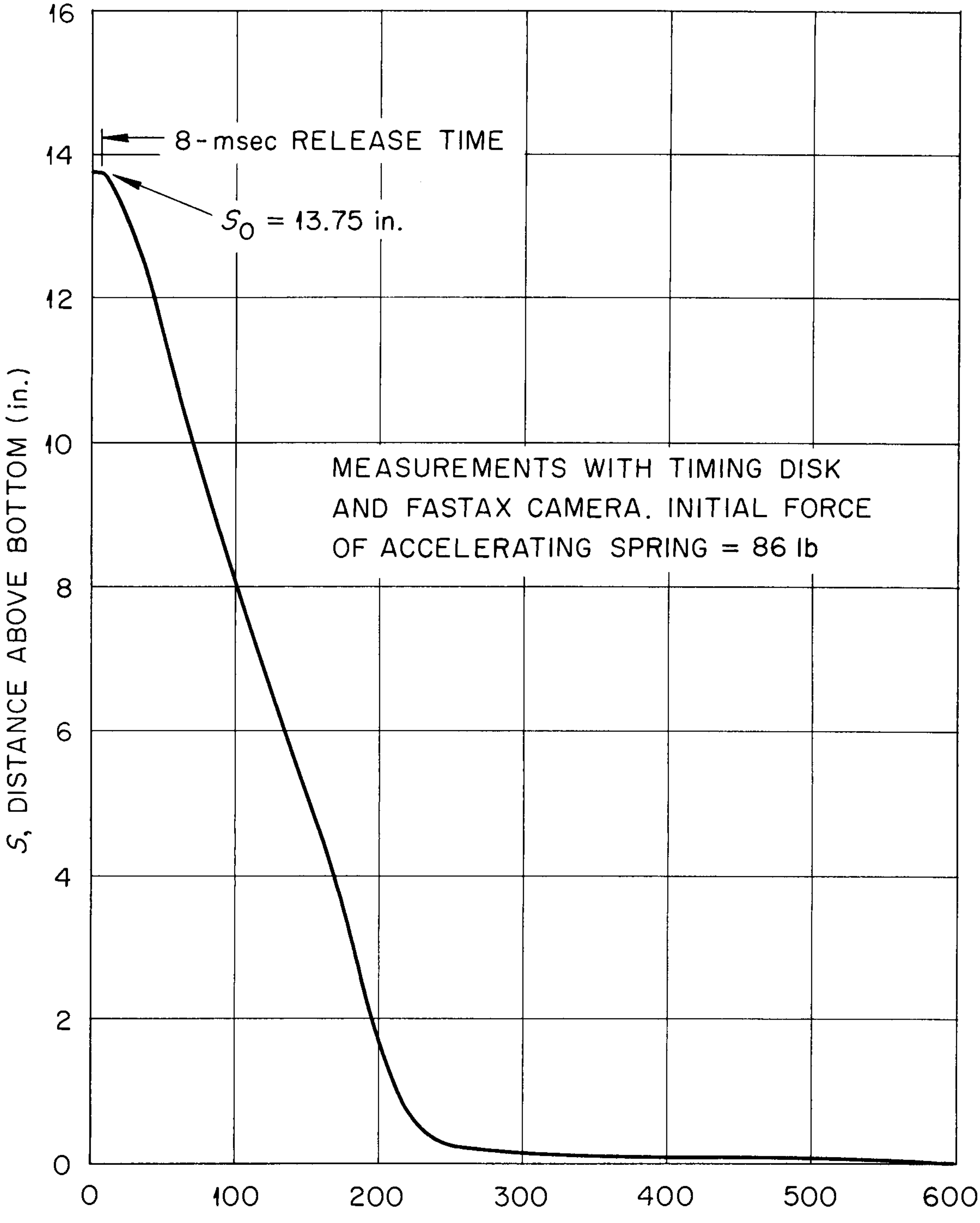

Fig. 26. Position of BSR-II Control Plate Lower Edge as a Function of Time After Start of Drop, as Measured with Timing Disc and Fastax Camera. The accelerating spring had an initial force of 86 lb.

Prompt neutron lifetimes of 10, 15, 20, and 25 μsec were simulated to cover the probable range of the experimental value to be measured later. However, considerations discussed in the body of this report indicate that even the maximum lifetime simulated is conservative, i.e., shorter than the reactor neutron lifetime. Therefore, simulation of larger neutron lifetime cases is planned. However, for evaluation of the safety aspects of the control system the conservative assumption calculations reported here suffice. Maximum control plate withdrawal corresponds to 1-in. insertion on the sensitivity curve. This initial position was used in the following determinations given in Table 5.

In Figs. 27 and 28 solitary points are plotted for comparison for the case of gravity rod drop in water, $a = 20$ ft/sec^2, at the initial plate position of 1-in. insertion. The results on these two figures are plotted from additional data taken to show the effects of control plate worth and control plate upper limit settings upon minimum period protection. In all tests, the period figures stated apply to a maximum power overshoot of three decades occurring during control plate insertion following a scram signal. The maximum excess reactivity figures are calculated from the inhour equation as those amounts necessary to initiate the periods indicated in the tables.

The simulation diagram of the corrective action is illustrated in Fig. 29.

Table 5. Period and Excess Reactivity Associated with a Transient Excursion of a Factor of 10^3 Obtained by Analog Simulation of the BSR-II Control System for Various Reactor Conditions

Prompt Neutron Generation Time, ℓ^* (μsec)	Total Reactivity Worth of the Control Plates (%)									
	4%		6%				8%		10%	
	66-lb Initial Spring Force		66-lb Initial Spring Force		86-lb Initial Spring Force		66-lb Initial Spring Force		66-lb Initial Spring Force	
	Period, τ (msec)	$\Delta k/k$ (%)	Period, τ (msec)	$\Delta k/k$ (%)	Period, τ (msec)	$\Delta k/k$ (%)	Period, τ (msec)	$\Delta k/k$ (%)	Period, τ (msec)	$\Delta k/k$ (%)
25	7.8	1.06	6.4	1.13			6.0	1.17	5.8	1.19
20	7.5	1.03	6.3	1.08	6.2	1.09	5.8	1.11	5.5	1.14
15	7.1	0.96	6.2	1.01	6.0	1.02	5.6	1.03	5.4	1.04
10	6.9	0.91	5.8	0.94	5.6	0.94	5.3	0.96	5.0	0.96

UNCLASSIFIED
2-01-058-0-372

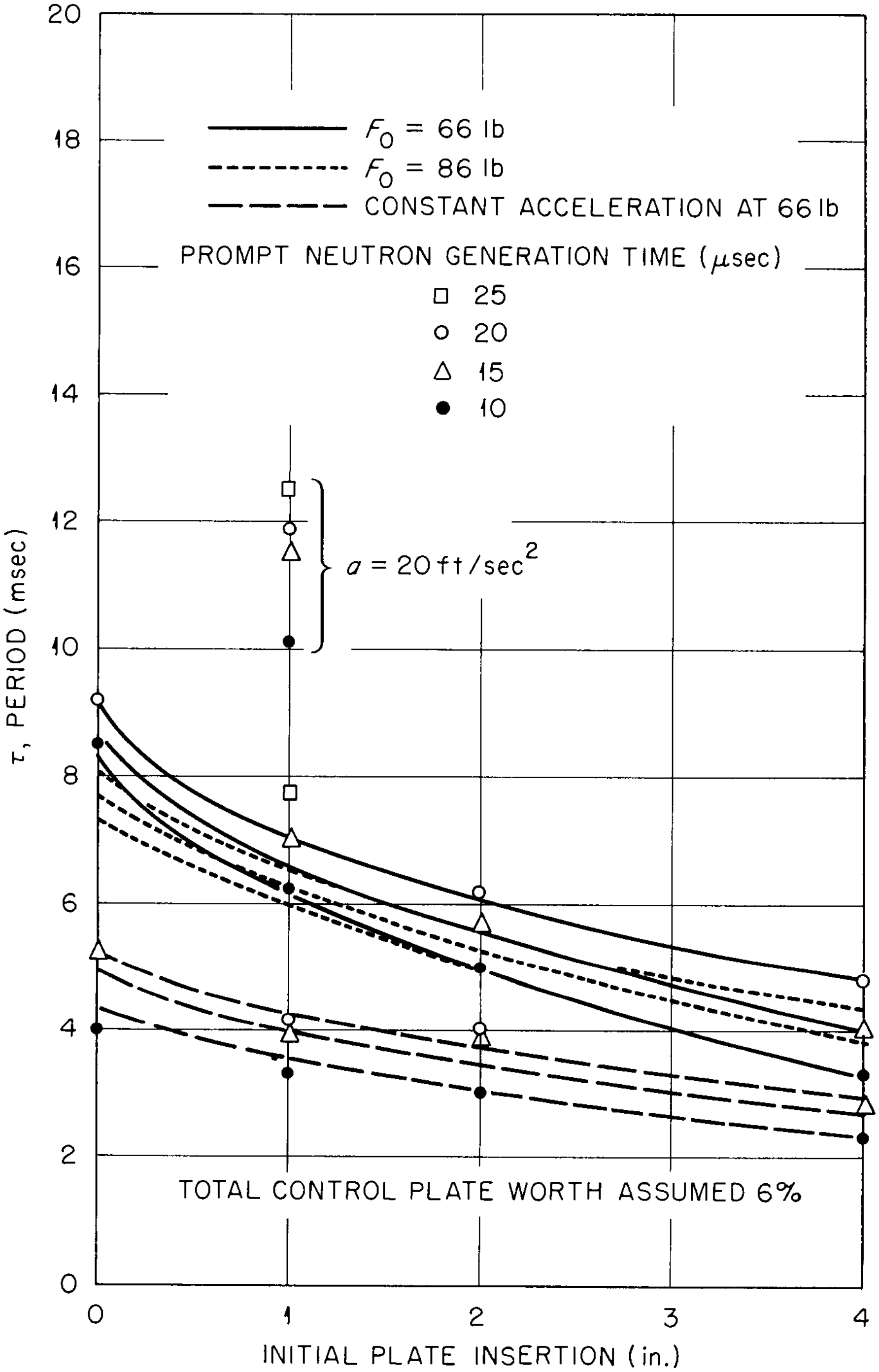

Fig. 27. Period, τ, in Millisec that can be Reversed Within a Flux Rise of a Factor of 10^3 by the BSR-II Control System, as a Function of Initial Insertion of Control Plates. Totol control plate worth is assumed to be 6%, and various prompt neutron generation times from 10 to 25 microsec are considered. The solid curves represent the result with a spring of initial force of 66 lb, the dotted curves represent the result using a spring of 86 lb initial force, and the dashed lines represent the result assuming uniform acceleration with a force of 66 lb during the entire stroke.

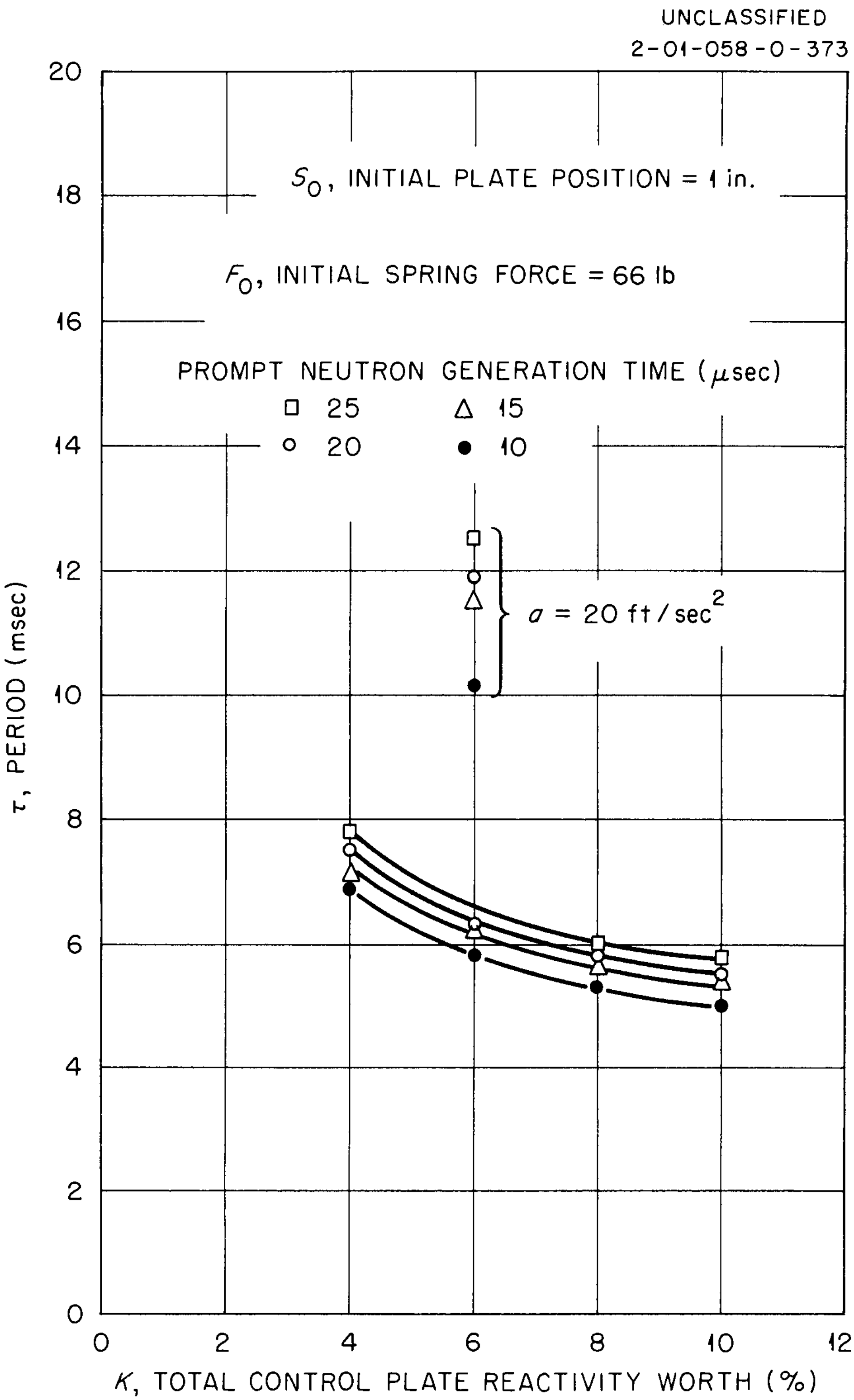

Fig. 28. Period, τ, that can be Reversed Within a Three Decade Power Excursion by the BSR-II Control System for Various Prompt Neutron Generation Times, and with an Accelerating Spring of 66 lb, Initial Force; Shown as a Function of Total Reactivity Worth of the Control Plates.

UNCLASSIFIED
2-01-058-0-374

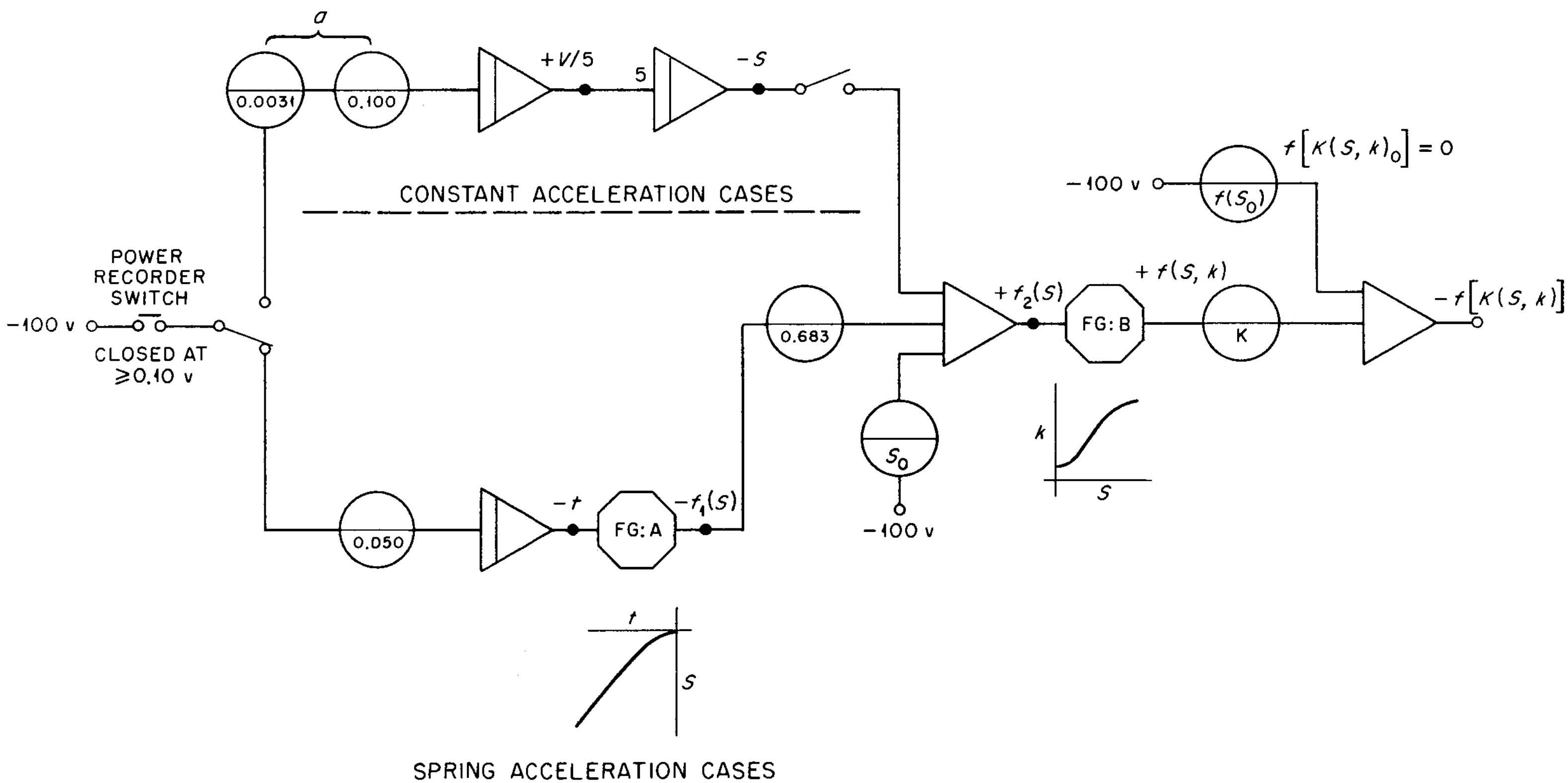

Fig. 29. Block Diagram of the Analog Computer Simulation of the BSR-II Control System and Reactor Response. The symbols represent anolog components, as defined by F. P. Green[10] or C. L. Johnson.[11]

Appendix 7

AFTER-HEATING IN AIR

The calculation of the temperature rise in the BSR-II due to fission-product heating after shutdown has been carried out on the basis of an extrapolation of an experiment carried out by K. M. Henry *et al.*[12] on a single BSR-I fuel element.

The experiment proceeded as follows: A single fuel element was exposed so that the power level for the element was 0.035 Mw for a period of 263 min. The element was then quickly withdrawn into an air chamber above the reactor core, and the temperature of several points on the fuel plates observed. Heat loss from the element through its support was estimated to be negligible. Figure 30 shows the temperature history at the hottest point observed. This point was 10 in. up from the bottom of the middle fuel plate. The dip in the temperature at about 12 min is judged to be due to loss of the adhering water film by rapid evaporation. The maximum temperature this point of the element reached was 102°C, at a time 43 min after withdrawal into the air space.

In order to extrapolate from this experimental information to the case of the BSR-II, a calculation was made of the heat transfer from the BSR-I element at the time of its maximum temperature. With this information the heat transfer in the central BSR-II element was calculated on the basis of two different models of the heat transfer mechanism.

At the instant of constant temperature in the experimental element this element was producing heat at a rate of 877 Btu/hr. This number is

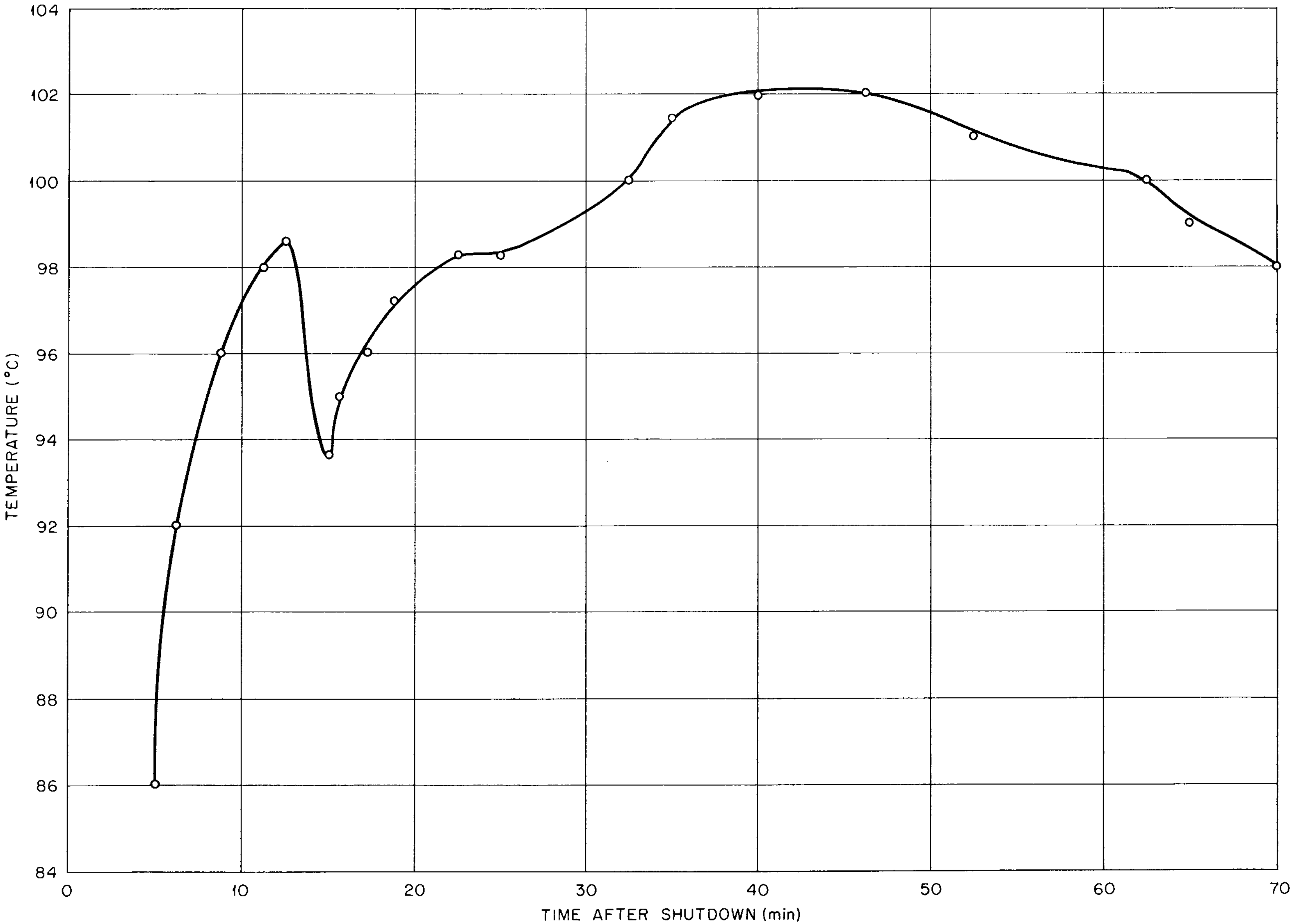

Fig. 30. Temperature 10 in. from Lower End of a Fuel Plate Suspended in Air Immediately Following Removal from a BSR-I Fuel Element. Fuel element had been operating at a power of 0.035 Mw for 4 hr 23 min.

obtained from the Way-Wigner formula which states that the heat produced t seconds after shutdown following operation at power P for time T seconds is given by:

$$Q = cP\left[t^{-0.2} - (t + T)^{-0.2}\right] \text{ Btu/hr}$$

The quantity cP was estimated to be 1.3×10^4 Btu/hr on the basis of an experiment performed on the LITR.[13] This equation yielded the result of 877 Btu/hr at the time of temperature equilibrium.

In the experimental element heat was lost not only by convection in the interior air passages, but also from the outer surface. The heat loss rate from the latter effect was calculated by the equation:

$$Q_{ext} = Ah_c\,\Delta T$$

where

A = surface area, ft^2,

h_c = heat transfer coefficient given by $h_c = 0.162\,\Delta T^{0.25}$ according to McAdams' "Heat Transmission" for the case of a warm plate facing a cold one,

ΔT = temperature difference between the element and the surrounding container.

This yields a heat loss rate of 130 Btu/hr.

The heat dissipated through the interior channels at the time of equilibrium was therefore 747 Btu/hr.

Two models were then used for the calculation of the temperature in the BSR-II element. First the assumption was made that a film coefficient for heat transfer could be stated as $h = k\Delta T^{0.25}$, leading to an equation of the form

$$Q_{ch} = kA\Delta T^{1.25}$$

Using this equation with a value of $k = 0.1045$ determined from the experiment with the BSR-I, a temperature vs. time curve for the case of the BSR-II central element was constructed by a step-wise approximation to the differential time behavior of the system. The time after shutdown was divided into intervals of 50 sec, and the heat produced during each interval calculated by integrating the Way-Wigner equation. The heat loss during each interval was conservatively estimated by assuming it to be governed by the temperature at the beginning of the interval and assuming it to be given by the equation above. Dividing the net heat-content change by the thermal capacity of the system, a temperature change during each interval was calculated, and the new temperature used as initial temperature for the next interval.

This step-wise procedure was carried out under two assumptions:

1. Operation for an infinite length of time at full power prior to shutdown; 15-sec delay before withdrawal of water.
2. 20-hr operation at full power prior to shutdown; 15-sec delay before withdrawal of water.

The effect of the adhering film of water was taken into account by calculating the power produced during the time of the temperature dip in the

BSR-I experiment, the heat taken up in cooling the element, and the heat leakage during the same time interval. After allowing for the smaller surface area of the BSR-II element, a result of 55 Btu removed by water film evaporation in the BSR-II element was obtained; this is equivalent to a 52°F temperature drop, and this was subtracted in the time interval during which the temperature passes the boiling point of water.

The maximum temperatures reached after shutdown in the center element of the BSR-II were found to be according to

Assumption 1: 450°C at 19.5 min after shutdown,

Assumption 2: 305°C at 15.2 min after shutdown.

These numbers are far below the melting point of steel at about 1400°C, and they represent conservative calculations, since the assumption that the test element was uniformly at the highest temperature measured leads to an underestimate of the heat transfer coefficient, and thus an overestimate of the temperature. Radiative and conductive heat losses were also neglected.

The second model for the heat transfer from the elements is based on the assumption that the air flow rate through the channels, rather than the film transfer coefficient, limits the convective heat loss. In this model it was assumed that the air in the channel reaches equilibrium with the metal temperature in the channel and that the temperature profile is the same in both the BSR-I and BSR-II elements.

Using this model one arrives at the following expression for the heat flow from a single fuel channel:

$$Q_{ch} \approx VC\lambda\beta(\Delta T)$$

where

V = flow velocity, in ft/hr, given by:

$$V \approx \frac{b^2}{\mu}\left[\frac{1}{T_1} - \frac{1}{T_2}\right]$$

b = plate separation distance, ft,

μ = viscosity of the air, assumed to be proportional to the upper air temperature, cp,

T_1 = air inlet temperature, $^{\circ}F$,

T_2 = metal temperature,[14] $^{\circ}F$,

C = flow area of the channel, ft^2

= ab, where a is the channel width,

λ = air density at the high, or metal temperature, proportional to $1/T_2(^{\circ}R)$, lb/ft^3,

β = specific heat of air, Btu/lb, assumed to be constant,

$\Delta T = T_2 - T_1$.

Combining these terms one arrives at an expression for the heat loss from the element given by the equation:

$$Q_{ch} = \frac{kab^3(\Delta T)^2}{(T_1)(T_2)^3} N \quad \text{(Btu/hr)}$$

where

N = the number of interior channels per fuel element.

As in the previous case, k was obtained from the BSR-I experiment, and a step-wise calculation was made of the temperature of the BSR-II central fuel element. The same two assumptions concerning the prior operating history were made as in the calculations with the first heat transfer model. The results for the maximum temperature of the central fuel element are:

Assumption 1: $263^{\circ}C$ at 10.25 min after shutdown,

Assumption 2: $177^{\circ}C$ at 7.75 min after shutdown.

It is therefore concluded, on the basis of the experimental extrapolation described here, that there is no danger of a fuel element melt-down in case of coolant loss from the elements immediately after shutdown if air is permitted to circulate through the BSR-II core by natural convection.

Appendix 8

MECHANICAL STRESS CALCULATIONS

To calculate the stresses to which the fuel elements and control elements of the BSR-II will be subjected under applied forces, it is necessary to obtain the moments of inertia about the axis of symmetry of the cross section of the fuel element. The element may then be considered to be a beam with this moment of inertia, fixed at one end and subject to a lateral load at the other. The formula for the stress at a point k inches from the free end of the beam is:

$$S = \frac{FCk}{I}$$

where

F = applied force, lb,

S = stress, lb/in.^{2},

C = distance from the neutral axis to the furthest fiber, in.,

k = distance between the end of the beam and the point where the stress is wanted, in.,

I = moment of inertia of the cross section of the beam about the neutral axis and perpendicular to the direction of the applied force, in.^{4}

It is evident from the equation above that the maximum stress in the plates occurs at the point at which the side plates are welded to the lower end box. Table 7 gives the calculated moments of inertia applicable to the calculation of the maximum force permissible within the elastic limits of the fuel elements. The moment calculation does not take the fuel plates into account, since these are not attached to the lower end box and therefore do not contribute to the strength at the junction point. The force needed to cause yielding at the lower end box fitting was then calculated assuming a yield strength of type 347 stainless steel of 30,000 lb/in.^{2} So:

$$F = \frac{30{,}000I}{Ck}$$

where the symbols are defined as in the previous equation. The results are quoted in the body of the report.

In order to calculate the deflection of the control plate element as a result of the force applied laterally, the equation for a beam loaded at one end and fixed at the other is used. This equation is:

$$\partial = \frac{Fk^3}{8EI}$$

where

∂ = deflection of the end of the beam, in.,

F = lateral force on the free end of the beam, lb,

k = length of the beam, in.,

E = elastic modulus of the material lb/in.^{2}

and I is defined above. In applying this calculation to the control plate

Table 7. Calculated Moments of Inertia of BSR-II Fuel and Control Plate Elements

	Moments of Inertia (in.^{4})	
	Standard Fuel Element	Control Fuel Element
I^*_{xx}	0.646	0.444
I_{yy}	0.224	0.858

*The x-axis is defined to be parallel to the side plates.

element of BSR-II for loads perpendicular to the control plate channel, the effect of fuel plates on the moment of inertia was included, since these plates do stiffen the element against bending. However, only the cladding of the fuel plates was included, since the "meat" portion has insignificant strength.

The moment of inertia, including the fuel plate cladding material, is $I_{xx} = 1.218 \text{ in.}^4$ The deflection needed to produce binding was calculated to be 0.046 in. in the worst case, i.e., if the control plate has the maximum thickness permitted by the dimensional tolerances, and the channel has the mimimum width permitted. The average value of the deflection required to produce binding is 0.059 in. The force is thus found to be:

$$F = \frac{3EI\delta}{k^3} = \frac{0.046 \times 29 \times 10^6 \times 1.218}{(16.94)^3} = 995 \text{ lb}$$

in the case of mimimum clearance.

The calculation of the deflection caused by concentrated force against the center of the cover plate over the control plate channel was carried out by a method given by Timoshenko.[15] In the calculation it was assumed that the plate is a rectangle simply supported at all edges. The effect of the free ends is negligible in the case under consideration, as will be shown below.

The deflection $w(x,y)$ at any point (x,y) of a rectangular plate simply supported at the edges under a concentrated load P at point (λ,γ) is given by:

$$w(x,y) = \frac{4P}{\pi^4 abD} \sum_{m=1}^{\infty} \sum_{n=1}^{\infty} a_{m,n} \sin \frac{m\pi x}{a} \sin \frac{n\pi y}{b}$$

where

$$a_{m,n} = \frac{1}{\left(\frac{m^2}{a^2} + \frac{n^2}{b^2}\right)^2} \sin \frac{m\pi\lambda}{a} \sin \frac{n\pi\gamma}{b}$$

The other terms are defined as follows:

$w(x,y)$ = deflection from the unstressed position, in.,

P = load, lb,

a = length of the plate in the x direction (plate extends from $x = 0$ to $x = a$), in.,

b = width of the plate in the y direction (plate extends from $y = 0$ to $y = b$), in.,

D = "flexural rigidity" given by $Eh^3/12(1 - \nu^2)$,

E = elastic modulus, lb/in.^{2},

ν = Poisson's ratio, taken to be 0.3.

λ and γ are the x and y coordinates of the point where the load P is applied. In the special case under consideration here, the load is applied at the center; therefore $\lambda = a/2$, $\gamma = b/2$, and the deflection at the center is desired. The equations then reduce to:

$$w\left(x = \frac{a}{2}, y = \frac{b}{2}\right) = \frac{4P}{\pi^4 abD} \sum_{m=1,3,5\ldots}^{\infty} \sum_{n=1,3,5\ldots}^{\infty} \frac{1}{\left(\frac{m^2}{a^2} + \frac{n^2}{b^2}\right)^2}$$

The following numbers were used in the calculation:

$$a = 2.89 \text{ in.}$$

$$b = 15.75 \text{ in.}$$

$$h = 0.025 \text{ in.}$$

$$E = 29 \times 10^6 \text{ lb/in.}^2$$

w(maximum permissible deflection) = 0.046 in.

The result is a force, P, of 14 lb. In this case the ratio of length to width of the plate, b/a, is 15.75/2.89 = 5.45. Timoshenko points out[16] that the difference between the result calculated for a rectangular plate and one for an infinitely long plate diminishes rapidly as the ratio of b/a increases. This difference is of the order of 0.5% for a ratio of b/a = 5. Therefore, in the case considered, the effect of the ends of the plate is negligible, and the fact that these are not supported will not affect the result of the calculation.

If it is assumed that the plate is rigidly clamped at all edges, rather than simply supported as was supposed above, then an equation given by Timoshenko[17] may be used for a completely built-in rectangular plate; this equation is:

$$w_{center} = \alpha \frac{Pa^2}{Eh^3}$$

where the quantities are defined as previously, and P is a force applied at the center of the plate. The coefficient, α, is a function of the ratio b/a, and becomes almost constant for b/a greater than 2. The case under discussion is therefore essentially the case of an infinite plate, and the free ends do not perturb the result appreciably. The value of α is 0.0788, which leads to the result that the force to deflect the plate sufficiently to bind the control plate is 53 lb.

The case of force distributed along the centerline of the control plate was also calculated. In this case the plate may be considered to be a beam of thickness 0.025 in., width 15.75 in. and span 2.891 in. Again assuming simple support, the formula[18]

$$w = \frac{Pk^3}{48EI}$$

applies. Here P is the load in pounds applied at the center of the beam, k is the span of the beam in inches, E is the modulus of elasticity, and I is the moment of the beam about the neutral axis of the cross section of the beam. I is given by:

$$I = \frac{ah^3}{12}$$

where

a = the width (15.75 in.),

h = the thickness (0.025 in.).

The result of this calculation is 54 lb to deflect the plate 0.046 in., which is the deflection that will produce binding of the control plate. If the assumption is made that the plate is rigidly held at the welds, then the case of a beam with built-in ends and a center load is represented. In this case the equation[19]

$$w = \frac{Pk^3}{192EI}$$

applies. The quantities are identical to those defined for the previous equation, and the result is 210 lb to cause binding of the control plate.

REFERENCES

1. "The Oak Ridge National Laboratory Research Reactor Safeguard Report Volume II - Appendix," F. T. Binford, Ed. App. m. p. 69 (Oct. 7, 1954) (Classified).

2. Op. cit. App. n, p. 87.

3. Op. cit., Volume I, Sec. 7f, p. 59.

4. K. M. Henry and J. N. Anno, "Appl. Nuclear Phys. Ann. Rep. Sept. 10, 1956," ORNL-2081, p. 25.

5. F. T. Binford, op. cit., ORNL-1794, Vol. I, Sec. 8, p. 60.

6. F. G. Prohammer, "A Comparison of One-Dimensional Critical Mass Calculations with Experiments for Completely Reflected Reactors," ORNL-2007 (Mar. 16, 1956).

7. E. G. Silver, ORNL-2081, op. cit., p. 47.

8. S. Glasstone and M. C. Edlund, "The Elements of Nuclear Reactor Theory," D. Van Nostrand, Inc., New York, 1952.

9. E. B. Johnson, K. M. Henry, J. D. Kington, and A. B. Reynolds, "Appl. Nuclear Phys. Ann. Rep. Sept. 1, 1957," ORNL-2389, p. 3.

10. F. P. Green, "ORNL Reactor Controls Analog Facility - Operating Manual," ORNL-2405 (to be published).

11. C. L. Johnson, "Analog Computer Techniques," McGraw-Hill, New York, 1956.

12. K. M. Henry and J. N. Anno, "Element After Heating," ORNL-CF-55-11-94 (Nov. 1955).

13. S. E. Beall, "An Experimental Determination of Fission Product Heating After Shutdown of the LITR," ORNL-1075, (Sept. 1951).

14. W. K. Stromquist, "Heat Dissipation from Fuel Assemblies of High Flux Reactor After Shutdown," ORNL-120 (Oct. 16, 1948) (declassified).

15. S. Timoshenko, "Theory of Elastic Stability," pp. 314-316, McGraw-Hill, New York, 1936.

16. S. Timoshenko, "Theory of Plates and Shells," p. 158, McGraw-Hill, New York, 1940.

17. Op. cit., pp. 222-231.

18. F. B. Seely, "Resistance of Materials," Third Edition, p. 161, John Wiley and Sons, New York, 1947.

19. Op. cit., Problem 297, p. 170.

20. F. Schroeder, S. G. Forbes, W. E. Nyer, F. L. Bentzen, and G. O. Bright, "Experimental Study of Transient Behavior in a Subcooled, Water-Moderated Reactor," Nuclear Science and Engineering, 2, 96-115 (1957).

ACKNOWLEDGEMENT

We wish to acknowledge the assistance of Francis P. Green, who carried out the analog calculations on which the kinetic behavior analysis of BSR-II is based. We are also grateful to the members of the ORNL Controls Division, and especially to A. Sorenson, who was on loan to that division from the Martin Company, for assistance with the control plate drop tests. The help of E. B. Johnson and K. M. Henry, who performed the control plate experiments with the BSR-I, is also gratefully acknowledged, as well as the work of V. Kelly, who, while on loan from the Martin Company, did much of the detailed mechanical design for this reactor.

ORNL-2470
Reactors-General
TID-4500 (13th ed. Rev.)

INTERNAL DISTRIBUTION

1. C. E. Center
2. Biology Library
3. Health Physics Library
4-5. Central Research Library
6. Reactor Experimental Engineering Library
7-26. Laboratory Records Department
27. Laboratory Records, ORNL R.C.
28. A. M. Weinberg
29. L. B. Emlet (K-25)
30. J. P. Murray (Y-12)
31. J. A. Swartout
32. E. H. Taylor
33. E. D. Shipley
34. M. L. Nelson
35. M. T. Kelley
36. C. P. Keim
37. J. H. Frye, Jr.
38. W. H. Jordan
39. R. R. Dickison
40. F. L. Culler
41. S. C. Lind
42. A. H. Snell
43. A. Hollaender
44. K. Z. Morgan
45. T. A. Lincoln
46. A. S. Householder
47. R. S. Livingston
48. D. S. Billington
49. C. E. Winters
50. D. W. Cardwell
51. D. Phillips
52. G. E. Boyd
53. J. A. Lane
54. M. J. Skinner
55. E. P. Blizard
56. C. W. Angel
57. R. J. Beaver
58. C. J. Borkowski
59. A. D. Callihan
60. R. A. Charpie
61. C. E. Clifford
62. G. deSaussure
63. S. Ditto
64. E. P. Epler
65. R. M. Farnham
66. S. H. Hanauer
67. K. M. Henry
68. L. B. Holland
69. E. B. Johnson
70. J. Lewin
71. J. D. Kington, Jr.
72-87. F. C. Maienschein
88. L. C. Oakes
89. R. W. Peelle
90. M. E. Ramsey
91-93. E. G. Silver
94. E. O. Wollan
95. H. P. Yockey
96. F. L. Friedman (Consultant)
97. H. Goldstein (Consultant)
98. H. Hurwitz, Jr. (Consultant)
99. L. W. Nordheim (Consultant)
100. R. R. Wilson (Consultant)
101. ORNL - Y-12 Technical Library, Document Reference Section

EXTERNAL DISTRIBUTION

102-131. H. M. Roth, AEC, Oak Ridge